PAPER

Check for updates

Synergistic impacts of nanopollutants (nZnO) and hypoxia on bioenergetics and metabolic homeostasis in a marine bivalve *Mytilus edulis*†

Fangli Wu, [iD] [abc] Eugene P. Sokolov,[b] Stefan Timm[d] and Inna M. Sokolova [iD] *[be]

Coastal ecosystems face increasing threats from anthropogenic pollution and environmental stressors like hypoxia and nanoparticle exposure. The Baltic Sea exemplifies these challenges due to nutrient pollution and hypoxia. We investigated the combined effects of zinc oxide nanoparticles (nZnO), which possess unique properties such as high reactivity and bioavailability, and hypoxia on bioenergetics and metabolite homeostasis of the blue mussel *Mytilus edulis* from the Baltic Sea. Mussels were first exposed to environmentally relevant concentrations of nZnO (100 μg Zn L^{-1}) and subsequently subjected to short-term (24 h) or long-term (7 d) hypoxia (<0.1% air saturation) followed by recovery periods (1 h and 24 h). Our findings reveal complex effects of nZnO on mussel metabolism under normoxic and hypoxic conditions. Under normoxic conditions, nZnO alters mussel metabolism without causing energy deficit. Prolonged severe hypoxia induces anaerobic metabolism and glycogen depletion. Under hypoxic conditions, nZnO disrupts mussels' metabolic response to anaerobic conditions, threatening their anaerobic survival capacity. Control mussels swiftly recover metabolic homeostasis upon reoxygenation, whereas nZnO-exposed mussels show delayed recovery, with ongoing energy disturbances. Overall, these findings underscore the metabolic impacts of nZnO and hypoxia in keystone marine mussels and emphasize the importance of considering oxygen levels in assessments of nanoparticle toxicity in coastal ecosystems.

Environmental significance

Our research on the metabolic responses of the mussel *Mytilus edulis* to zinc oxide nanoparticles (nZnO) and hypoxia has significant environmental implications. nZnO, known for its hazardous potential, can disrupt marine ecosystems by causing toxicity in keystone species like blue mussels. Our study reveals how nZnO, when combined with hypoxia, intensifies metabolic stress and delays metabolic recovery, threatening organism survival and therefore ecosystem stability. By elucidating these interactions, our work is crucial for assessing the impact of nanopollutants under realistic environmental conditions. It underscores the necessity of incorporating nanoparticle-induced metabolic disruptions into coastal environmental risk assessment.

1. Introduction

Coastal areas are highly productive and dynamic ecosystems vulnerable to the combined effects of multiple stressors like climate change, ocean acidification, urbanization and pollution. Anthropogenic pollution is a major contributor to the environmental risks faced by coastal ecosystems.[1] Nutrient pollution from agricultural runoff, sewage discharge, and industrial activities induces eutrophication, causing oxygen depletion (hypoxia) and biodiversity loss, especially in enclosed basins like the Baltic Sea.[2–5] Chemical pollutants, notably nanoparticles such as nano-ZnO, further challenge coastal environments, entering *via* various pathways like wastewater, urban runoff, transport and recreational activities, potentially endangering marine life and ecosystem stability.[6–9] The interplay of these stressors complicates coastal ecology and environmental risk assessment, with poorly understood cumulative effects on marine organisms necessitating further research.[2,10]

Metabolism plays a key role in integrating the impacts of various stressors on organisms, adjusting metabolic pathways

[a] SCNU Environmental Research Institute, Guangdong Provincial Key Laboratory of Chemical Pollution and Environmental Safety & MOE Key, Laboratory of Theoretical Chemistry of Environment, South China Normal University, Guangzhou, 510006, China

[b] Department of Marine Biology, Institute for Biological Sciences, University of Rostock, Rostock, Germany. E-mail: inna.sokolova@uni-rostock.de

[c] School of Environment, South China Normal University, University Town, Guangzhou, 510006, China

[d] Department of Plant Physiology, Institute for Biological Sciences, University of Rostock, Rostock, Germany

[e] Department of Maritime Systems, Interdisciplinary Faculty, University of Rostock, Rostock, Germany

† Electronic supplementary information (ESI) available. See DOI: https://doi.org/10.1039/d4en00479e

576 | *Environ. Sci.: Nano*, 2025, **12**, 576–596

This journal is © The Royal Society of Chemistry 2025

to maintain cellular and organismal balance amidst environmental challenges like pollutants, temperature changes, and oxygen fluctuations.[11,12] This dynamic response involves altering energy production, nutrient utilization, and the synthesis of vital molecules essential for survival and stability.[11,13,14] Disruption to metabolism not only affects immediate physiological functions but also compromises overall fitness and resilience of the organism. Stress-induced metabolic imbalance can deplete energy reserves, hinder growth, impair reproductive success and weaken immune defenses, heightening susceptibility to disease and predation.[11,12,15,16] Diminished individual fitness due to metabolic disruptions can jeopardize population viability and alter community dynamics, with ramifications at both the population and ecosystem levels.[17]

Hypoxia, or oxygen deficiency, poses a significant metabolic challenge to aerobic organisms, including marine benthic animals. In the absence of oxygen, mitochondrial respiration, responsible for over 90% of cellular ATP production under normal conditions, ceases, and the less efficient anaerobic pathways are activated for ATP generation.[18,19] This transition to less efficient anaerobic ATP generation can lead to severe energy deficits and the accumulation of metabolic waste, disrupting cellular balance and potentially causing cell death.[20–23] Some benthic marine organisms, like the blue mussels *Mytilus edulis*, have evolved a survival strategy called metabolic rate suppression to endure short-term hypoxia. This involves slowing down both ATP production and consumption, conserving energy reserves and reducing waste accumulation to delay cellular imbalance.[18,24,25] While this adaptation allows mussels to recover quickly after hypoxia events, the shift to anaerobic metabolism still disrupts energy balance and intermediary metabolism, which can only be fully restored upon reoxygenation.[26–30] The restoration of metabolic homeostasis during reoxygenation comes at a significant energy cost to the organism, reflected in elevated respiration rates (known as oxygen debt), and is accompanied by increased production of reactive oxygen species (ROS), which can further damage cellular components.[31–35]

Anthropogenic pollutants, including industrial chemicals, pesticides and nanoparticles, disrupt normal metabolic processes, leading to physiological dysregulation and potential health and ecological impacts.[13,36,37] Nano-zinc oxide (nZnO), released from various industries and products such as sunscreens, cosmetics, and paints, poses significant concerns in coastal marine ecosystems due to its small size, high surface-to-volume ratio, reactivity, and high predicted environmental concentrations, as well as ability to accumulate in the sediment and biota.[38,39] Studies have reported that predicted environmental concentrations of nZnO reach hundreds of ng L^{-1} in European natural surface waters[39–42] and up to 100 μg L^{-1} in polluted areas.[39,40,43] These particles are taken up by aquatic organisms, causing toxicity through mechanisms such as oxidative stress, immune perturbations, inflammation, and

cytotoxicity.[6,9,44–46] Recent studies also suggest metabolic disturbances in various organisms exposed to nZnO,[47–49] but its effects on marine invertebrates' metabolism and interactions with other stressors like hypoxia are poorly understood.

Our study aimed to investigate how environmentally relevant concentrations of nZnO (100 μg L^{-1}) affects the bioenergetics and metabolic responses of the Baltic Sea blue mussel *M. edulis* to short-term (24 h) and long-term (7 d) severe hypoxia and subsequent reoxygenation. The nZnO concentration of 100 μg L^{-1} was chosen based on its use in previous sub-lethal exposure studies in marine bivalves, and its relevance to the environmental concentrations predicted in polluted areas.[39,40,43] The blue mussels *M. edulis*, a filter feeder, encounters nanoparticles through water, diet, and suspended sediments.[50,51] With increasing hypoxia in the Baltic Sea coastal zone, lasting from hours to weeks,[5] *M. edulis* serves as an ideal model to study the combined effects of nZnO and hypoxia on metabolism. Here, we hypothesized that nZnO exposure would impair mitochondrial aerobic capacity, exacerbate hypoxia-induced metabolic stress, and delay recovery in *M. edulis*. To test these hypotheses, we assessed whole-body energy status using the Cellular Energy Allocation (CEA) approach[52,53] and mitochondrial capacity through measuring mitochondrial electron transport chain (ETS) activities, citric synthase (CS) enzyme activity, and mitochondrial DNA copy number in mussel soft tissues. Metabolic profiling focused on free amino acids, anaerobic end products, TCA cycle intermediates, and urea cycle intermediates using liquid chromatography coupled with tandem mass spectrometry (LC-MS/MS). Our findings shed light on novel toxic mechanisms of nZnO as a metabolic disruptor in a keystone marine species, the blue mussel *M. edulis*.

2. Materials and methods

2.1 Animal collection and acclimation

In February 2021, adult blue mussels *M. edulis* were collected near Rostock, Germany in the Baltic Sea (54°10′49.602″N, 12°05′21.991″E). The mussels had a soft body wet weight of 3.2 ± 0.7 g and a shell length of 54.9 ± 4.0 mm. The habitat salinity and temperature at the collection site were 9–15 (practical salinity scale) and 5–10 °C, respectively. Within 2 h of collection, the mussels were transported to the University of Rostock in a cooler. The mussels without shell damage were chosen for experiments after cleaning the epibionts on the shell surface. Before the experimental exposures, the mussels were laboratory-habituated for two weeks in a recirculating temperature-controlled aquarium at salinity 15 and temperature 10 °C. Two weeks are considered sufficient to reach physiological steady-state after an environmental shift in temperate mussels.[54,55] The mussels were continuously fed a commercial blend of live algae *Nannochloropsis oculata*, *Phaeodactylum sp.* and *Chlorella sp.* (Premium Reef Blend, CoralSands, Wiesbaden, Germany)

This journal is © The Royal Society of Chemistry 2025

Environ. Sci.: Nano, 2025, 12, 576–596 | 577

based on the manufacturer's instructions throughout the experiment unless otherwise indicated.

2.2 Characterization of nZnO nanoparticles

The nZnO used in this study was obtained from Sigma-Aldrich Sweden AB (Stockholm, Sweden), and its preparation and characterization were detailed in an earlier report.[46] Briefly, the average particle size was 30.1 ± 0.4 nm, a surface area of dry nZnO was 35 m^2 g^{-1}, the hydrodynamic size was 5.21 ± 0.21 μm and zeta potential was −16.0 mV for a nZnO suspension of 100 mg Zn L^{-1} at salinity 15 and 10 °C.[46] The data on Zn accumulation in soft tissue of mussels corresponding to normoxic conditions in the present study, which indicated a significant Zn accumulation ($P < 0.05$) at 100 μg L^{-1} of nZnO, has been reported elsewhere.[56] Prior to the addition of nZnO to the experimental seawater, the stock suspension of nanoparticles (10 mg L^{-1} Zn) was sonicated for 20 min and added to vigorously aerated experimental tank seawater to achieve the target concentration (100 μg L^{-1} Zn).

2.3 Experimental exposures

The mussels used for this study were from the same experimental exposures described in our earlier report.[57] The experiment included two factors (nZnO concentration and dissolved oxygen (DO) regime) in a fully crossed design. Two concentrations of nZnO (0 and 100 μg L^{-1} Zn) and five DO regimes, including normoxia (~90–100% of air saturation), short- and long-term hypoxia (1 and 7 d at ~0.1% of air saturation), as well as short- and long-term reoxygenation (1 and 24 h reoxygenation following 7 d of hypoxia), were used. For the sake of brevity, mussels not exposed to nZnO will be referred to as control mussels, and those exposed to 100 μg L^{-1} Zn as nZnO as nZnO-exposed mussels. The nZnO concentration of 100 μg L^{-1} was chosen based on its use in previous sub-lethal exposure studies in marine bivalves, and its relevance to the environmental concentrations predicted in polluted areas.[39,40,43] Short- and long-term severe hypoxia (1 and 7 d at ~0.1% air saturation) were selected to simulate possible scenarios that mussels may encounter in eutrophicated estuaries and coastal dead areas during seasonal hypoxia,[58–61] and are consistent with methodologies employed in previous studies.[62] Two recovery periods (1 and 24 h) were chosen because the molecular and cellular stress responses associated with reoxygenation usually occur within minutes to hours after oxygen recovery.[33,63–65]

The mussels were exposed to two treatments (control and nZnO exposure) for 21 d, with artificial filtered seawater changed every two days and feeding before each water change. The 21 d exposure period was chosen because it allows marine bivalves to achieve a new physiological steady-state after an environmental shift.[54,55] Each treatment consisted of three replicate tanks with 76–77 mussels per tank (25 L seawater). In the nZnO-exposed groups, a suspension of nZnO was added after each water change throughout the experiment, including the hypoxia and

reoxygenation periods. After 21 d exposure, subsets of randomly chosen mussels from the two experimental treatment groups (control and nZnO-exposed) were exposed to three different oxygen conditions (normoxia, 1 d hypoxia, and 7 d hypoxia). Each treatment consisted of three replicate chambers with 13–14 mussels and 1.5 L of seawater per chamber. The DO content in all treatments was monitored using a FireStingO$_2$ optical oxygen meter and a fiber optic oxygen sensor (PyroScience GmbH, Aachen, Germany). Because the mussels closed their shells and stopped feeding in hypoxia, we did not add food to the hypoxia-exposure chambers to minimize bacterial growth. For reoxygenation, a subset of mussels from the 7 d hypoxia group was randomly chosen and transferred to a fully aerated water tank for 1 and 24 h. Each treatment consisted of three replicate tanks (25 L of seawater per tank) with 13–14 mussels per tank for control treatments and 6 mussels for nZnO treatment. All experimental treatments were conducted at 10 °C and salinity 15 in a 12 : 12 light : dark regime. After experimental exposures, the entire soft body of the mussels was immediately collected and shock-frozen, ground under liquid nitrogen and stored at −80 °C until further analyses.

2.4 Condition index (CI)

The CI was calculated as the ratio of the soft tissue mass to the shell volume, where the shell volume (cm^3) was calculated as the product of shell length, shell width, and shell height (cm).[66]

2.5 Tissue content of energy-rich compounds

Colorimetric methods were used to measure the concentrations of lipids, carbohydrates, and proteins in whole-body homogenates of mussels.[67] A standard colorimetric method was employed to measure lipid concentrations using chloroform-methanol extraction.[68] Protein concentrations were determined with the Biorad Bradford Protein Assay Kit using bovine serum albumin as a standard, according to the manufacturer's instructions. The phenol-sulphuric acid method was used to measure carbohydrate concentrations.[69] Further information on the analyses can be found in our previous report.[46] A SpectraMax ID3 Multi-Mode Microplate Reader was used to determine the absorbance of lipids, proteins, and carbohydrates at 490 nm, 595 nm, and 492 nm, respectively. Lipid and protein concentrations were expressed in mg g^{-1} wet mass, while carbohydrate concentrations were expressed as μmol glucose equivalents g^{-1} wet mass.

2.6 Mitochondrial activity and abundance

The spectrophotometric 2-(4-iodophenyl)-3-(4-nitrophenyl)-5-phenyl tetrazolium chloride (INT) reduction assay[67,70] was used to measure electron transport system (ETS) activity in the whole soft body extracts of the mussels using a SpectraMax ID3 multi-mode microplate reader (Molecular Devices, USA) at 20 °C. For blank reading, 0.7 mM KCN and

578 | Environ. Sci.: Nano, 2025, 12, 576–596

This journal is © The Royal Society of Chemistry 2025

10 μM rotenone were added to inhibit ETS and determine the non-mitochondrial reduction of INT-tetrazolium. The rate of formazan formation was used to calculate the specific ETS activity of the tissues (μmol O_2 min^{-1} mg wet tissue mass) based on an extinction coefficient of 15.9 mM^{-1} cm^{-1} at 490 nm and corrected for the light path (0.523 ± 0.023 cm). The ETS activity was calculated as the difference in the activity in the absence and presence of the ETS inhibitors, and expressed as nM O_2 min^{-1} g^{-1} wet tissue mass using the stoichiometric equivalent of 1 μmol formazan to 0.5 μmol O_2.

The cellular energy allocation (CEA) was calculated as the ratio of total energy content to the potential energy expenditure.[71] To determine the total energy reserve of the mussels, the measured protein, lipid, and carbohydrate content was converted into energy equivalents, using their respective energy of combustion: 24 kJ g^{-1} for proteins, 39.5 kJ g^{-1} for lipids, and 17.5 kJ g^{-1} for carbohydrates.[72] The potential energy expenditure was calculated based on the ETS flux using oxyenthalpic equivalents for the combustion of an average mixture of lipids, glycogen, and proteins (484 J $mmole^{-1}$ O_2).[72,73]

Citric synthase (CS) activity assay in whole-body homogenates of mussels was adapted from the method outlined elsewhere.[74] In brief, free coenzyme A production was tracked using 5,5′-dithiobis-(2-nitrobenzoic acid) (DTNB) by measuring the increase in absorbance at 412 nm. Background deacylase activity in the absence of oxaloacetate (OAA) was subtracted from the total activity. The reaction mixture included 0.5 mM OAA, 0.25 mM DTNB, 0.4 mM acetyl CoA, in 75 mM Tris-HCl buffer at pH 8.0, maintained at room temperature (approximately 20 °C). Reactions were initiated by addition of OAA.

Relative abundance of mitochondrial DNA (mtDNA) was determined as described elsewhere.[75] In brief, DNA extraction was carried out from ~20 mg of whole soft tissues using the E.Z.N.A. Mollusc DNA kit (Omega Bio-Tek, Norcross, GA, USA) following the manufacturer's guidelines. Quantification was performed spectrophotometrically using NanoVue Plus (GE Healthcare, UK), and samples were then diluted to 10–15 ng $μL^{-1}$ with TE buffer and re-quantified using SYBR Green I stain (MedChemExpress, Monmouth Junction, NJ, USA). Relative mitochondrial DNA (mtDNA) copy numbers were determined via real-time PCR against concurrently measured copy numbers of a single-copy nuclear gene. For mtDNA, coxI (NCBI AY484747.1) was amplified (forward primer: 5′ TATG CGGTGAGATGGACTGA, reverse primer: 5′ CCACAACGGCA TAGATAACCA), while for the nuclear gene, β-tubulin sequence (NCBI CAJPWZ010001239.1) was used (forward: 5′ AACAATATTTCACGGACCATCC, reverse: 5′ GAAGGTATCGA ACCTCCTCCTT). PCR was conducted using the StepOne Plus real-time PCR System and StepOne v2.3 software (Applied Biosystems). The qPCR reaction mixture consisted of Blue S'Green qPCR Master mix (Biozym Scientific, Oldendorf, Germany), 0.3 μM of each primer, and 10 ng of total DNA. Duplicate runs were performed for each sample. The thermal profile included an initial denaturation at 95 °C for 5 min, followed by 40 cycles of denaturation at 95 °C for 10 s, annealing at 55 °C for 20 s, and extension at 65 °C for 20 s. Ct values for the β-tubulin gene (Ct β-tub) and the mitochondrial coxI gene (Ct coxI) were determined for each sample within the same quantitative PCR run and averaged for technical replicates. Relative mtDNA copy number was calculated as Rc = 2 × $2^{\Delta Ct}$, where ΔCt = Ct β-tub − Ct coxI.

2.7 Metabolite analyses

Metabolite concentrations were measured by extracting 100 mg of whole soft tissue with 1 mL of 80% ethanol containing 1 μg mL^{-1} of 2-(N-morpholino)ethanesulfonic acid (MES) as an internal standard. The samples were centrifuged at 13 000 × g and 4 °C for 10 min. The supernatant was freeze-dried using the Unicryo MC2L (Martinsreid, Germany) at −60 °C and stored at −80 °C for further analysis. The extracts were dissolved in MS-grade distilled water (ROTISOLV® LC-MS-grade, Roth, Germany), filtered through 0.2 μm filters (Omnifix®-F, Braun, Germany) and analyzed using the LCMS-8050 system with electrospray ionization (ESI) as previously described.[29] A pentafluorophenylpropyl column (Supelco Discovery HS FS, 3 μm, 150 × 2.1 mm) was used for separation, and a consecutive gradient of 1 min 0.1% formic acid, 95% water, 5% acetonitrile, within 15 min linear gradient to 0.1% formic acid, 5% water, 95% acetonitrile, 10 min 0.1% formic acid, 5% water, 95% acetonitrile was used to elute the samples.

The LC-MS/MS method package for primary metabolites Ver. 2. (Shimadzu, P/N 225-24862-92) and the LabSolutions software package (Shimadzu, Japan) were used for the identification and quantification of metabolites.[29] The peak area (signal intensity) of the target compounds was normalized to the internal standard peak and calibrated with authentic standard substances (Merck, Germany) for each compound. The concentrations were expressed in μg g^{-1} wet mass of the soft tissue. Classification of amino acids as essential or non-essential was done based on the capacity for amino acid synthesis in mollusks, due to the limited knowledge of the specific amino acid biosynthesis pathways in Mytilus.[76] Amino acids with no biosynthetic capacity in mollusks (including Arg, His, Lys, Phe, Thr, Trp, and Val) or with the reported biosynthetic capacity in only some mollusks (Met, Ser, Ile, Leu, and Pro) were considered essential.[76] The remaining studied free amino acids (FAAs) were deemed non-essential.

2.8 Statistical analyses

IBM® SPSS® 18.0 and GraphPad Prism 6.0 were used for the data analysis. The normality of the data was checked before analysis using the Shapiro–Wilk's test, and homogeneity of variances was evaluated by Levene's test. For the non-normally distributed data, Box–Cox transformation was applied. The measured traits were analyzed using two-way ANOVA to evaluate the effects of nZnO treatment, dissolved oxygen (DO) regime, and their interactions. Tukey's HSD *post*

This journal is © The Royal Society of Chemistry 2025

Environ. Sci.: Nano, 2025, **12**, 576–596 | **579**

hoc multiple range tests were used to analyze the significant effects of dissolved oxygen treatments within each nZnO treatment, while Student's *t* test was used to analyze the significant effects of nZnO treatment at each fixed DO regime. For all measured traits, the results were expressed as means ± SEM, and a significance level of $P < 0.05$ was used to determine significant effects.

The impacts of oxygen regime and nZnO exposure on metabolism were analyzed using the pathway enrichment analysis as implemented in Metaboanalyst 5.0.[77] This analysis can identify subtle but consistent changes across compounds involved in the same biological pathway.[77] The regression approach was used to integrate metabolic changes after different durations of hypoxia (1 and 7 d) and different recovery periods (1 h and 24 h) relative to the normoxic controls. In the regression analyses, to avoid computational issues with zero values, the normoxic condition was assigned a very small non-zero value (0.0001 d of hypoxia exposure, or 0.0001 h of recovery). The citrate and isocitrate concentrations were treated together as citrate. Metabolic reference library of *Drosophila melanogaster* was used due to its extensive annotation and conservation of fundamental metabolic processes across species, with the Globaltest as the method of pathway enrichment analysis. The relative betweenness centrality was used as a node importance measure in the pathway topology analyses. The pathway was considered significantly enriched if the probability of the false discovery rate (FDR) was <0.05. Significantly enriched pathways (FDR < 0.05) with the pathway impact >0 were considered in the further analysis and discussion. Principal component analysis (PCA) was conducted to reduce the dimensionality of data set and visualize the changes in the integrated metabolite profiles in response to H–R stress using Metaboanalyst 5.0.[77] The correlation analysis and metabolite clustering were conducted in Metaboanalyst 6.0.[77] For correlation heat maps, the missing values for the protein content, ETS and CS activities (1–2 per group) were replaced with the respective group means. For pathway enrichment, PCA and correlation analysis, the concentrations of metabolites were autoscaled using means and standard deviations to normalize the data and minimize the effects of different scales for different compounds.

3. Results

3.1 Mortality and condition index (CI)

During normoxia and after 1 d of hypoxia, no mortality was found in mussels from control or nZnO exposures. After 7 d of hypoxia, 28% of control mussels and 63% of nZnO-exposed mussels died. After 24 h of reoxygenation, no mortality was observed in control mussels, and 11% of nZnO-exposed mussels died during reoxygenation (Table S1†). Exposure to nZnO or hypoxia–reoxygenation (H–R) stress had no effect on the condition index of the mussels ($P > 0.05$) (Fig. S1†).

3.2 Energy-rich compounds

Whole-body protein content was significantly higher in nZnO-exposed mussels compared with their control counterparts after 7 d of hypoxia and 1 h of recovery (Fig. 1A). There was a trend ($P > 0.05$) of decline in the body protein content during hypoxia followed by a rapid increase during reoxygenation (Fig. 1A). As a result, the whole-body protein content was significantly lower after 7 d of hypoxia relative to 24 h of recovery in both the control and nZnO-exposed groups (Fig. 1A).

Whole-body lipid content was similar in the control and nZnO-exposed mussels under the normoxic conditions (Fig. 1B). Lipid content declined after the prolonged (7 d) exposure to hypoxia in the nZnO-exposed (but not in the control) mussels (Fig. 1B).

In normoxia, the body content of carbohydrates (glycogen) was similar in the control and nZnO-exposed mussels (Fig. 1C). Glycogen content in the control mussels decreased after prolonged (7 d) hypoxia and recovered during reoxygenation reaching the normoxic baseline levels within 1 h of recovery (Fig. 1C). In nZnO-exposed mussels, the glycogen content of the body showed a decreasing tendency after 7 d of hypoxia and continued to decrease during reoxygenation reaching level significantly below the normoxic baseline. As a result, the body glycogen content of nZnO-exposed mussels after 1 h and 24 h of post-hypoxic recovery significantly lower than in their control (not exposed to nZnO) counterparts (Fig. 1C).

3.3 Mitochondrial activity and abundance

Activity of the mitochondrial ETS in the whole-body of *M. edulis* was suppressed by nZnO exposure under normoxic conditions as well as during hypoxia (Fig. 1E). Within each of the treatment groups (control or nZnO-exposed), there was no evidence of H–R-induced change in the ETS activity (Fig. 1E).

The baseline (normoxic) levels of CS were higher in the nZnO-exposed oysters compared to the controls (Fig. 1F). In the control mussels, CS activity increased during the prolonged (7 d) hypoxia exposure and remained elevated during 24 h of post-hypoxic recovery. In the nZnO-exposed mussels, CS activity was suppressed in hypoxia and returned to the baseline levels during the 1st h of post-hypoxic recovery (Fig. 1F).

The mitochondrial DNA copy number (mtDNA-CN) showed a slight, non-significant increase in mussels exposed to nZnO compared to the control group under normoxic conditions (Fig. 1G). No significant change in mtDNA-CN was observed after 1 d hypoxia. However, prolonged exposure (7 d) to hypoxia resulted in a marked decrease in mtDNA-CN in the control group (Fig. 1G). A modest reduction in mtDNA-CN was also noted after 7 d of hypoxia in the nZnO-exposed mussels, although this decrease did not reach statistical significance ($P > 0.05$) (Fig. 1G). Following 1 h of reoxygenation, mtDNA-CN remained suppressed in both
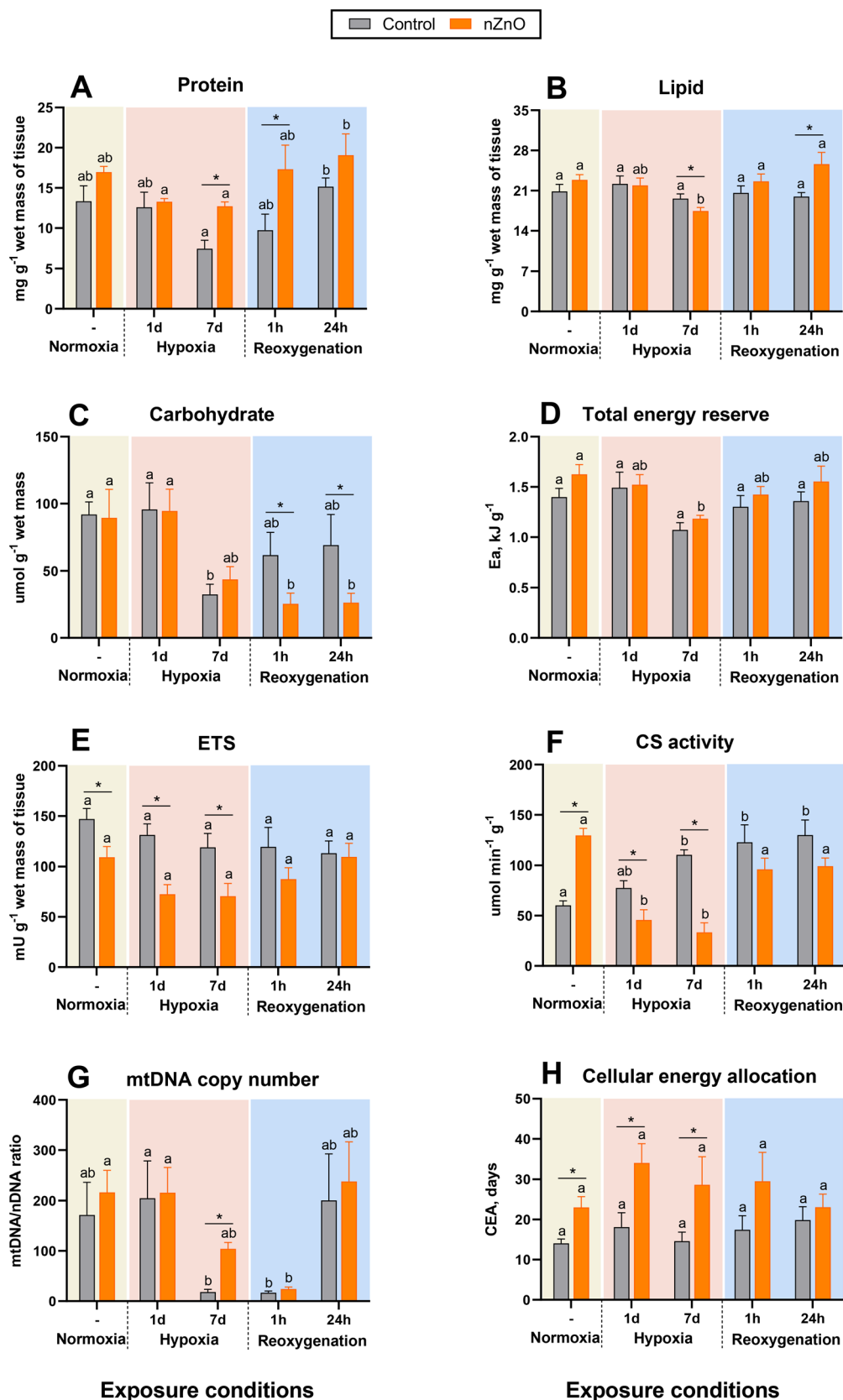
Fig. 1 Effects of hypoxia and nZnO exposure on bioenergetics parameters in the soft body of *M. edulis*. A – Protein, B – lipid, C – carbohydrate, D – total tissue energy content, E – ETS activity, F – CS activity, G – mitochondrial DNA copy number, H – cellular energy allocation (CEA). Different letters indicate values that are significantly different between different oxygen exposure conditions within the control or the nZnO-exposed group ($P < 0.05$). If the columns share a letter, the respective values are not significantly different ($P > 0.05$). Asterisks indicate significant differences between the control and nZnO-exposed group within the same oxygen treatment ($P < 0.05$). $N = 8$.

This journal is © The Royal Society of Chemistry 2025

Environ. Sci.: Nano, 2025, **12**, 576–596 | 581

experimental groups, recovering to baseline levels after 24 h (Fig. 1G).

CEA (reflecting the ratio of the total tissue energy content (Fig. 1D) and energy demand measured by ETS activity) was
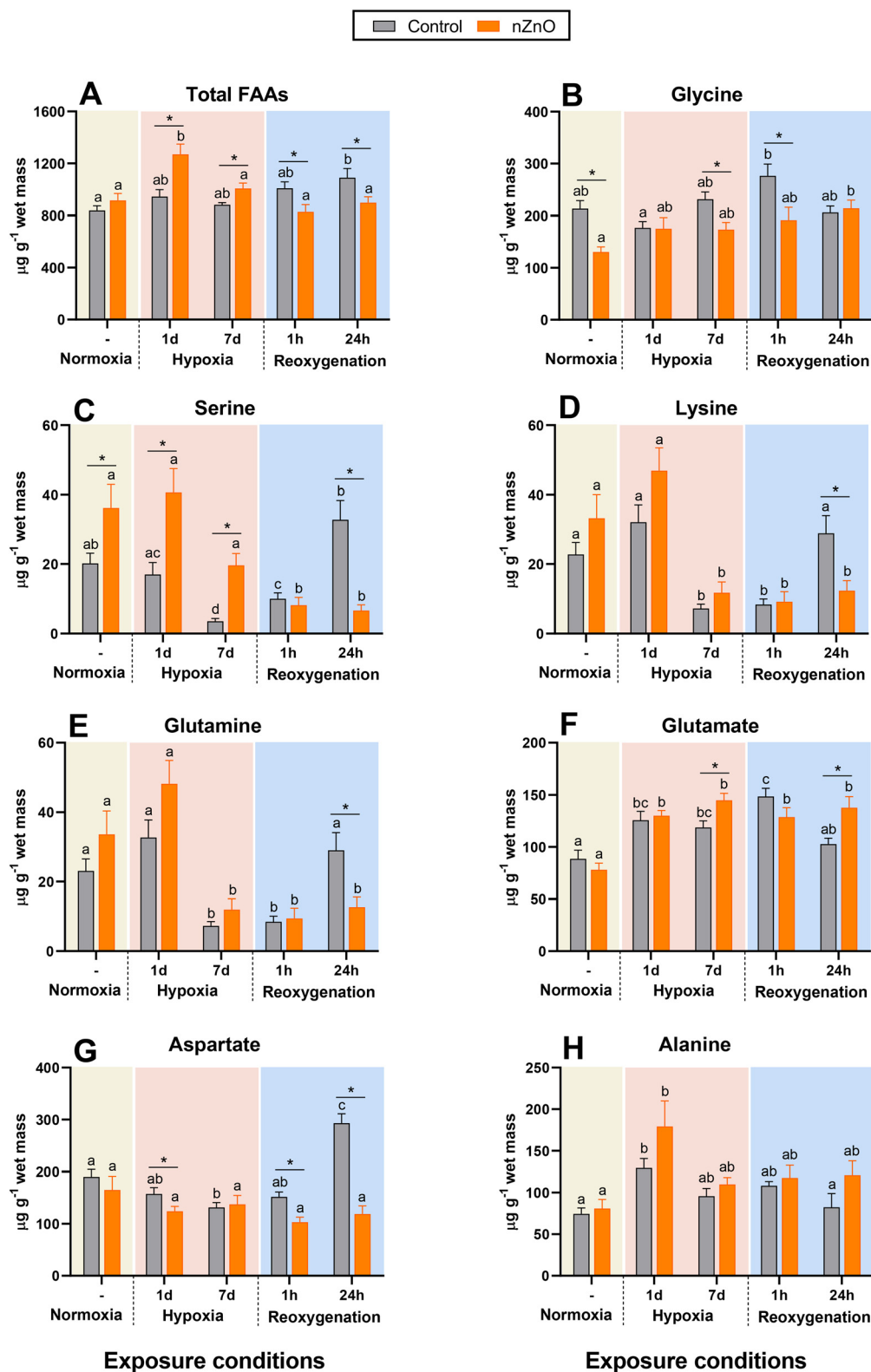

Fig. 2   Effects of hypoxia and nZnO exposure on the amino acid content in the soft body of *M. edulis*. A – Total free amino acids, B – Gly, C – Ser, D – Lys, E – Gln, F – Glu, G – Asp, H – Ala. For interpretations of letters and asterisks, see Fig. 1 caption. *N* = 8–10.

higher in the nZnO-exposed mussels compared to their control counterparts, and these differences were statistically significant in normoxia and hypoxia but not during the reoxygenation (Fig. 1H). In both control and nZnO-exposed groups, a strong negative correlation between CEA and ETS activity was found ($p < 0.05$) (Fig. S3†).

There was no consistent correlation between different mitochondrial biomarkers (ETS activity, CS activity and mtDNA-CN) in the mussel tissues (Fig. S3†). The ETS activity was positively correlated with the CS activity in the control mussels, but negatively – in their nZnO-exposed counterparts ($p < 0.05$). No significant correlation was observed between mtDNA-CN and ETS or CS activity in either group ($p > 0.05$) (Fig. S3†). Interestingly, in nZnO-exposed mussels, ETS activity was significantly positively correlated ($p < 0.05$) with the tissue levels of lipids and proteins, and negatively correlated ($p < 0.05$) with multiple metabolites including lactate, TCA intermediates (malate, citrate, fumarate, and succinate), FAAs (Glu, Lys, Ala, Met, Pro, Phe, Thr, Tyr, Val, Leu, Ile), MetO, and argininosuccinate (Fig. S3†). In control mussels, the only metabolite showing significant negative correlation with ETS activity was Met ($p < 0.05$) (Fig. S3†). No significant positive correlation of ETS activity with any of the studied traits was found in the control mussels.

3.4 Metabolite analyses

3.4.1. Free amino acids (FAAs) and their derivatives. Under normoxic conditions, several amino acids (including His, Arg, Trp, lactate, citrulline, fumarate, 2-oxoglutarate, 4-hydroxyproline, Ser, Leu, Phe, malate, (iso)citrate, succinate and argininosuccinate) and derivatives (MetO and 4-hydroxyproline) showed significant elevated levels in nZnO-exposed mussels compared to the controls (Table S2†). Gly levels were lower in nZnO mussels, while Asn, Asp, Ala, Thr, Pro, AMP, Tyr, GABA, carnithine, pyruvate, Glu, Gln, Lys, Val, Met, Ile, and ornithine showed no significant differences (Table S2†). Despite these variations, total FAAs levels were similar in nZnO-exposed and control mussels under normoxia (Fig. 2A and Table S2†).

The FAAs in control mussels remained stable during hypoxia and gradually increased during reoxygenation (Fig. 2A). The FAAs of nZnO exposed mussels increased by ~40% during the 1st d of hypoxia but then declined back to the normoxic baseline after 7 d of hypoxia and remained at the baseline during reoxygenation (Fig. 2A).

Glycine was the most abundant of the studied FAAs in the mussels' soft tissues (Fig. 2B and Table S2†). Under normoxic conditions Gly levels were higher in the control mussels relative to their nZnO-exposed counterparts (Fig. 2B). Gly did not change during H–R in control mussels and slightly but significantly increased after 24 h of reoxygenation in nZnO-exposed ones (Fig. 2B).

Ser, Lys and Gln in control mussels decreased after 7 d of hypoxia and remained suppressed after 1 h of reoxygenation, recovering back to the normoxic baseline after 24 h (Fig. 2C–

E). Changes in Ser, Lys and Gln in nZnO-exposed mussels followed a similar pattern, except that for the lack of recovery after 24 h of reoxygenation (Fig. 2C–E). Glu accumulated during hypoxia and the 1st h of recovery in both control and nZnO-exposed groups (Fig. 2F). After 24 h of recovery, Glu levels returned to the baseline in the control mussels but remained elevated in their nZnO-exposed counterparts (Fig. 2F).

Asp decreased during hypoxia in control mussels, and quickly recovered during reoxygenation with a significant overshoot after 24 h of recovery (Fig. 2G). In nZnO-exposed mussels, Asp did not change in response to H–R stress (Fig. 2G). Ala accumulated during the 1st d of hypoxia and returned to the baseline levels after 7 d of hypoxia and subsequent reoxygenation in both experimental groups (Fig. 2H).

Met, Val, Leu, Ile and Phe increased after 1 d of hypoxia in the control and nZnO-exposed mussels and remained elevated above the normoxic baselines throughout the H–R exposure (Fig. 3A–E). Hypoxia-induced accumulation of these amino acids was higher in nZnO-exposed mussels relative to their control counterparts (Fig. 3A–E).

MetO were consistently higher in nZnO exposed mussels in normoxia and during the H–R exposures, except after 24 h of recovery when a significant elevation in MetO in the control group equalized the MetO concentrations in control and nZnO exposed mussels (Fig. 3F).

Pro and 4-hydroxyproline accumulated after 1 d of hypoxia in nZnO-exposed mussels gradually returning to normoxic baseline after 7 d of hypoxia and reoxygenation (Fig. 4A and B). In control mussels, H–R exposure had negligible effect on Pro and 4-hydroxyproline (Fig. 4A and B). A similar pattern was found for Tyr, Trp and Thr; these amino acids accumulated during 1–7 d of hypoxia in nZnO-exposed mussels reverting to baseline levels post-reoxygenation, with no discernible alteration in response to H–R exposure in the control mussels (Fig. 4C–E).

His levels in nZnO-exposed mussels were high under the control conditions and after 1 d of hypoxia, gradually decreasing afterwards (Fig. 4F). No change in his content during H–R stress was found in the control mussels (Fig. 4F).

GABA accumulated in nZnO-exposed mussels during hypoxia and the 1st h of recovery but returned to baseline after 24 h of recovery (Fig. 4G). In control mussels, GABA levels remained stable throughout H–R exposure (Fig. 4G). Carnitine levels showed negligible change in throughout H–R exposures except for a decrease after 24 h of reoxygenation in nZnO-exposed mussels (Fig. 4H).

3.4.2. Glycolysis and TCA cycle metabolites. In control mussels, exposure to 1 and 7 d of hypoxia led to accumulation of succinate and 2-oxoglutarate (Fig. 5D and E). Hypoxia showed no effect on the tissue levels of pyruvate, lactate, fumarate, (iso)citrate or malate in the whole-body of the control mussels (Fig. 5A–C and F).

During post-hypoxic recovery of the control mussels, the tissue levels of most studied TCA intermediates (including succinate, fumarate, (iso)citrate, and 2-oxoglutarate), except
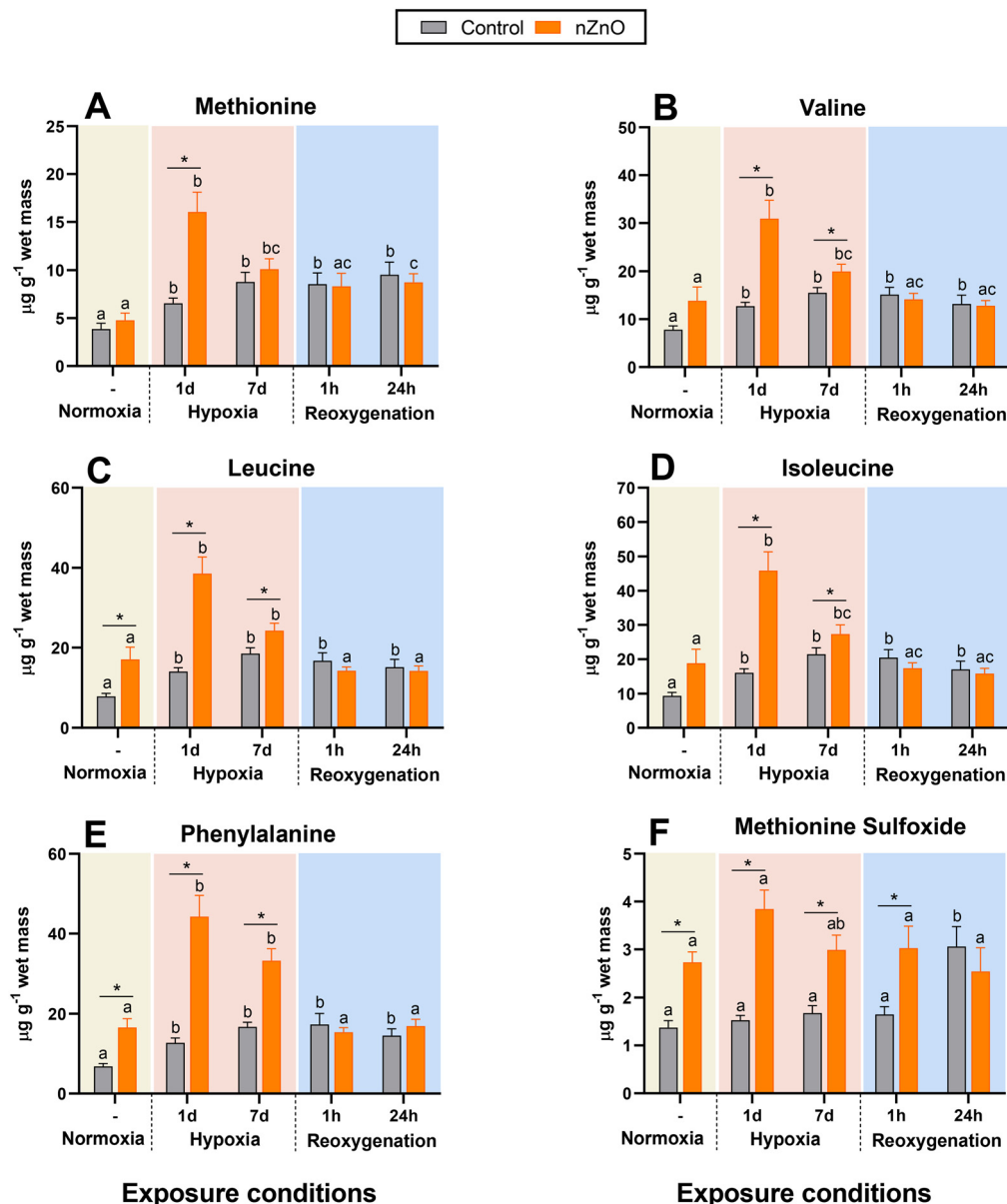
This journal is © The Royal Society of Chemistry 2025

Environ. Sci.: Nano, 2025, **12**, 576–596 | 583

Fig. 3 Effects of hypoxia and nZnO exposure on the amino acid content in the soft body of *M. edulis*. A – Met, B – Val, C – Leu, D – Ile, E – Phe, F – MetO. For interpretations of letters and asterisks, see Fig. 1 caption. N = 8–10.

malate, were significantly elevated above the normoxic baseline (Fig. 5). In the case of fumarate and succinate, this increase was transient and observed only after 1 h but not 24 h of recovery (Fig. 5E and F). There was no change in pyruvate, lactate, and malate concentrations in the recovering control mussels (Fig. 5A, B and G).

Under normoxic conditions, nZnO-exposed mussels showed elevated concentrations of TCA intermediates and lactate in their tissues compared with the tissues of the control counterparts (Fig. 5B–G). Exposure to nZnO interfered with the metabolic response to hypoxia as shown by the extremely high accumulation of succinate (after 1–7 d of hypoxia; Fig. 5E) and lactate (after 1 d of hypoxia; Fig. 5B) and lack of significant changes in any other studied TCA

intermediates (Fig. 5A, C, D and F) during hypoxia in nZnO-exposed mussels. During reoxygenation, tissue levels of pyruvate, lactate, (iso)citrate, 2-oxoglutarate, malate and fumarate returned to the normoxic baseline, whereas concentrations of succinate were elevated during reoxygenation in nZnO-exposed mussels (Fig. 5).

3.4.3. Urea cycle intermediates. Tissue levels of argininosuccinate, arginine and citrulline were elevated in nZnO-exposed mussels compared with the control ones under normoxic conditions, while the levels of ornithine did not differ between the two groups (Fig. 6). In control mussels, concentrations of most studied urea cycle intermediates remained stable under hypoxia (Fig. 6A, B and D), except for a modest increase in ornithine after 7 d of hypoxia (Fig. 6C).

584 | *Environ. Sci.: Nano*, 2025, **12**, 576–596
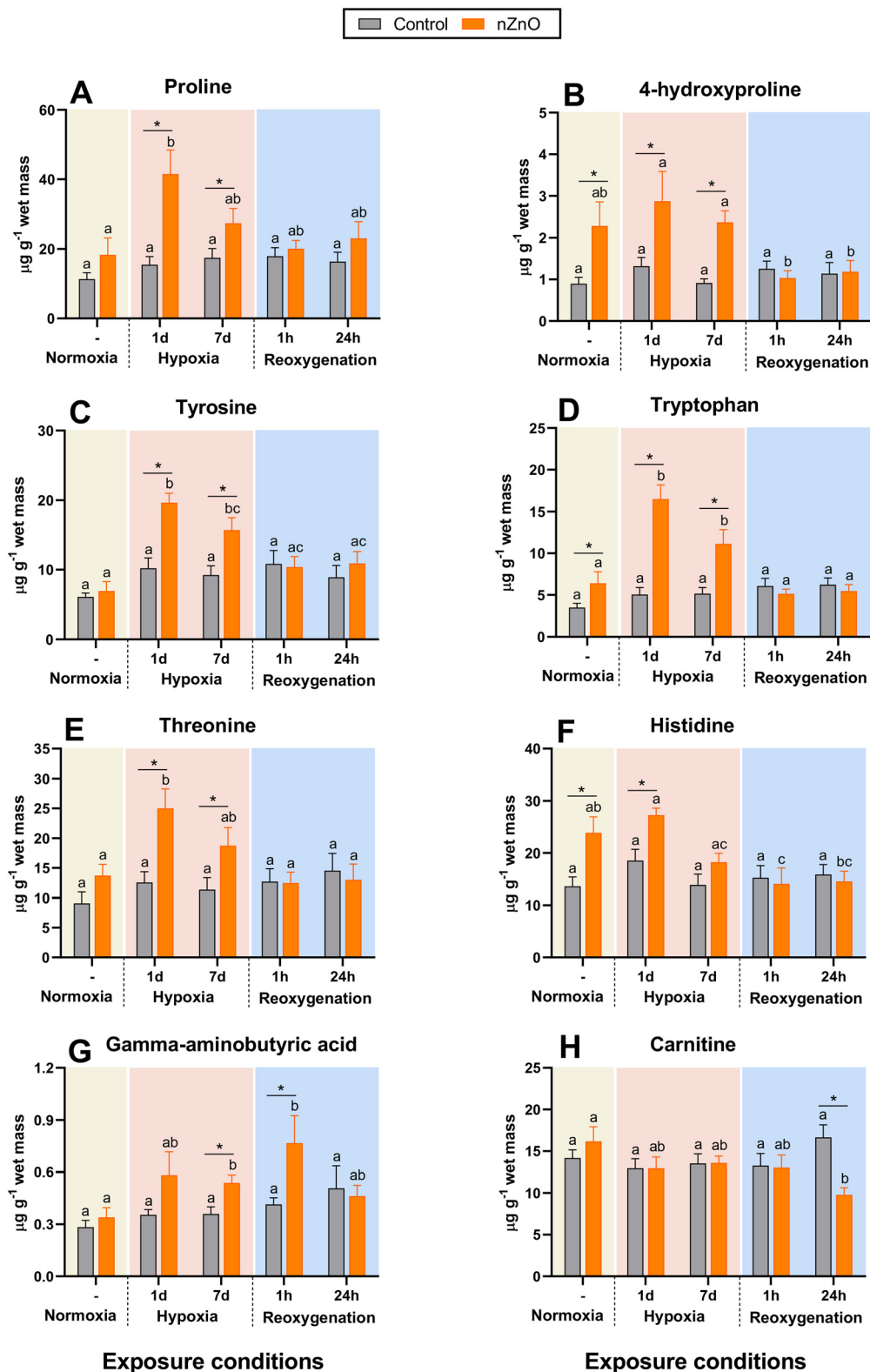
This journal is © The Royal Society of Chemistry 2025

Fig. 4 Effects of hypoxia and nZnO exposure on the content of amino acids and amino acid derivatives in the soft body of *M. edulis*. A – Pro, B – 4-hydroxyproline, C – Tyr, D – Trp, E – Thr, F – His, G – GABA, H – carnithine. For interpretations of letters and asterisks, see Fig. 1 caption. N = 8–10.

Reoxygenation resulted in accumulation of argininosuccinate in the control mussels, while tissue levels of other three studied intermediates returned to or remained at baseline (Fig. 6).
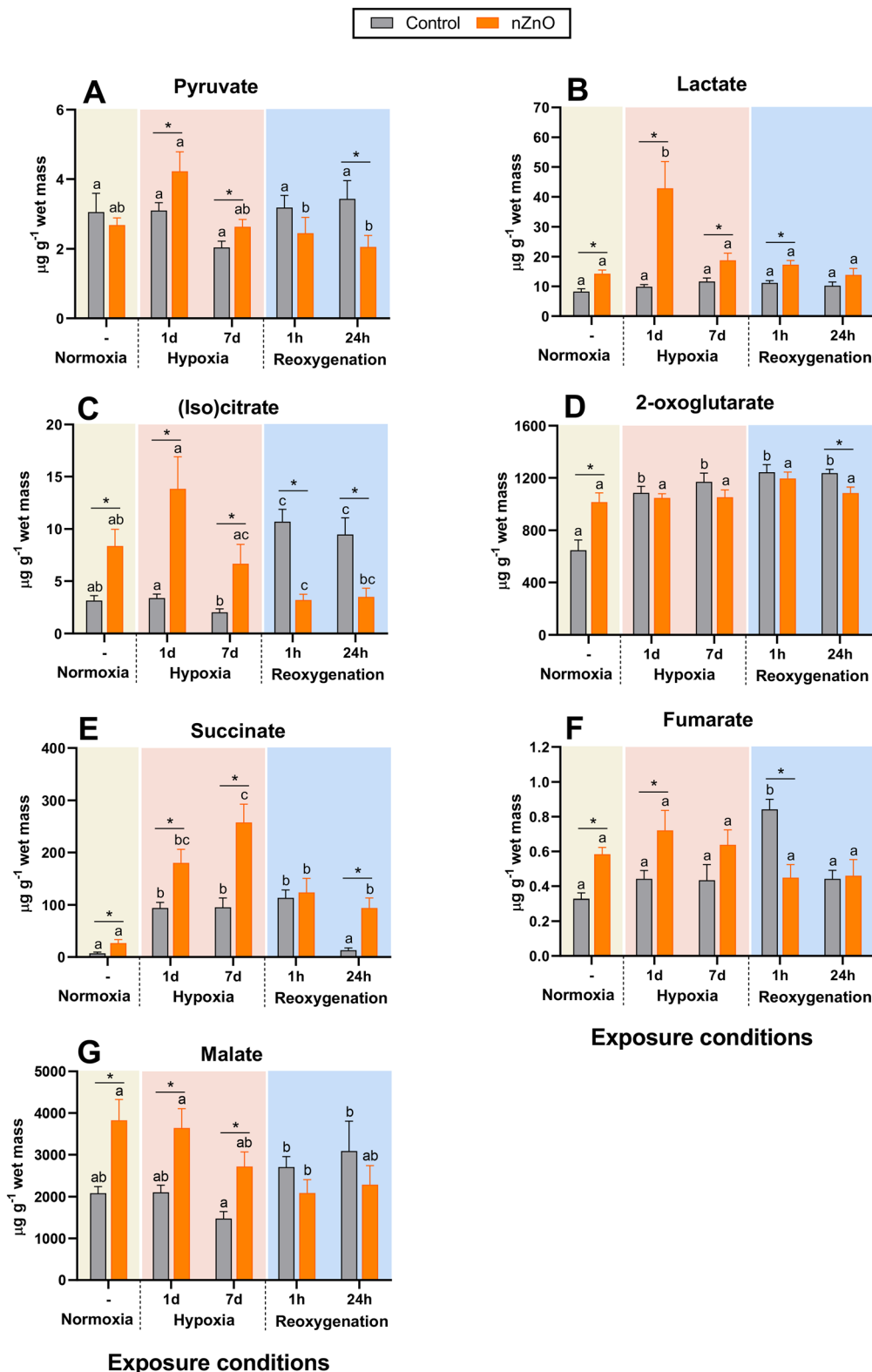
Fig. 5 Effects of hypoxia and nZnO exposure on intermediates of glycolysis and TCA cycle in the soft body of *M. edulis*. A – Pyruvate, B – lactate, C – (iso)citrate, D – 2-oxoglutarate, E – succinate, F – fumarate, G – malate. For interpretations of letters and asterisks, see Fig. 1 caption. $N = 8–10$.

In nZnO-exposed mussels, ornithine accumulated during 1 and 7 d of hypoxia, while the concentrations of argininosuccinate, arginine and citrulline remained at baseline (Fig. 6). Reoxygenation led to accumulation of ornithine and depletion of arginine and argininosuccinate in nZnO-exposed mussels (Fig. 6A–C).
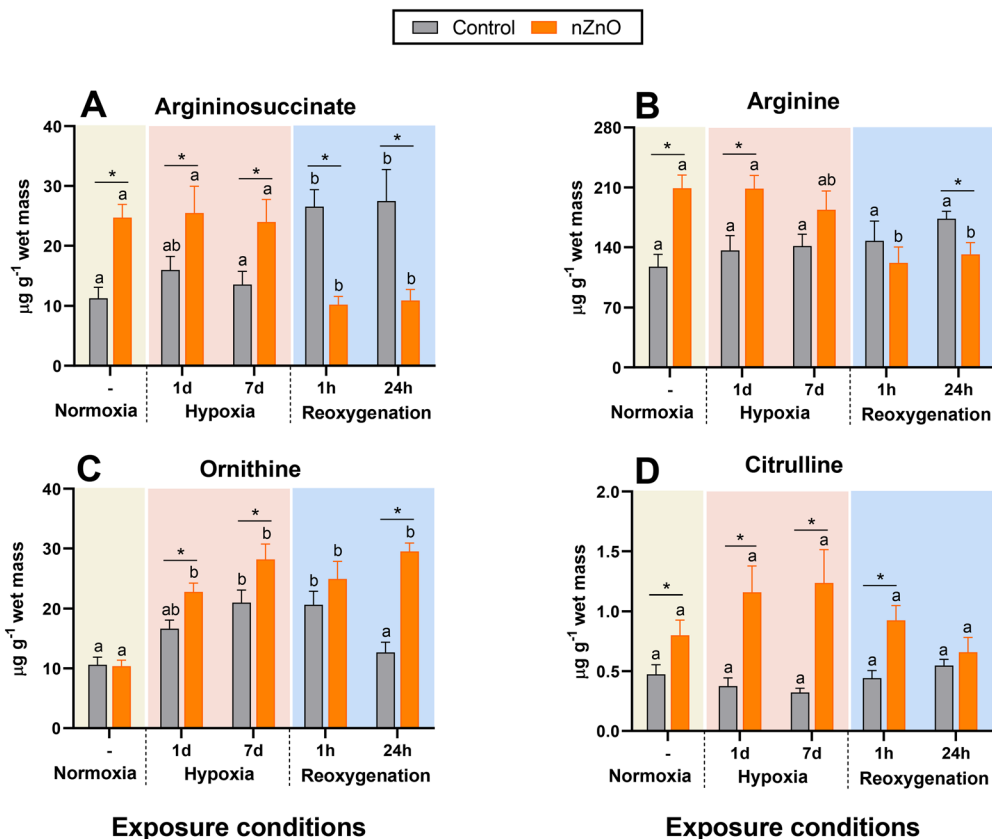
Fig. 6 Effects of hypoxia and nZnO exposure on the intermediates of urea cycle in the soft body of *M. edulis*. A – Argininosuccinate, B – Arg, C – ornithine, D – citrulline. For interpretations of letters and asterisks, see Fig. 1 caption. N = 8–10.
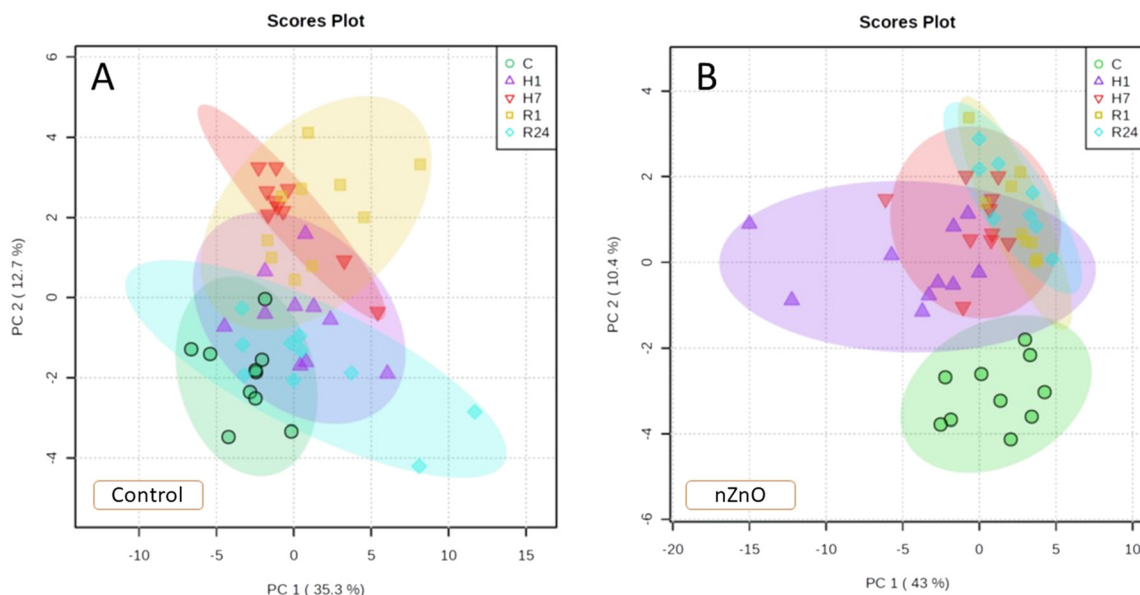

Fig. 7 PCA biplots showing positions of the metabolite profiles of control and nZnO-exposed mussels under different oxygen regimes. A – Control mussels, B – nZnO-exposed mussels. Oxygen regimes: C – normoxia, H1 – 1 d of hypoxia, H7 – 7 d of hypoxia, R1 – 1 h of reoxygenation, R24 – 24 h of reoxygenation. The ellipses indicate 95% confidence intervals for each group.

This journal is © The Royal Society of Chemistry 2025

Environ. Sci.: Nano, 2025, **12**, 576–596 | **587**

3.5 Integrated analyses of metabolite profiles

Under normoxic conditions, metabolite profiles of control and nZnO-exposed mussels were only partially separated in the plane of the two first PCA components jointly explaining 52% of data variation (Fig. S2A†). However, pathway enrichment analysis showed significant alterations in 12 pathways caused by nZnO exposure under normoxic conditions. These included arginine biosynthesis, TCA cycle, alanine, aspartate and glutamate metabolism, glyoxylate and dicarboxylate metabolism, glycine, serine and threonine metabolism, butanoate metabolism, pyruvate metabolism, tyrosine metabolism, histidine metabolism, arginine and proline metabolism, glutathione metabolism and D-glutamine and D-glutamate metabolism (Fig. S2B†).

PCA analysis of metabolites profile in control mussels identified two first principal components (PCs) jointly explaining 48% of the variation of the data set. The metabolite profiles of the mussels exposed to hypoxia were mostly separated from the control group along PC1 (35.3% variation, hypoxia axis), whereas the positions of the groups exposed to 1 and 24 h of reoxygenation were shifted relative to other groups along PC2 (12.7%, reoxygenation axis) (Fig. 7A). PC1 (hypoxia axis) had high positive loadings of Ala, Thr, Pro, Val, Met, Tyr, Ile, Leu, Phe and Trp (Table S3†). PC2 (reoxygenation axis) had high positive loadings of succinate, ornithine and Gly, and high negative loadings of Asp, Asn, Glu, Ser and Lys (Table S3†).

In nZnO-exposed mussels, the first two PCs explained 53.4% of the variation in metabolite concentrations. All experimental exposure groups (except for the mussels exposed to 1 d of hypoxia) showed considerable overlap along PC1 (43% of variation) (Fig. 7B). PC2 (10.4% of the variation) separated the control group from those exposed to hypoxia and reoxygenation (H–R axis). PC2 had high positive loadings of succinate, ornithine, Tyr, Glu and GABA and high negative loadings of Arg and Ser (Table S3†).

Correlation analysis revealed different relationships among the metabolite concentrations in the tissues of the control and nZnO-exposed mussels (Fig. S3†). Thus, in the whole body of the control mussels, three clusters of strongly positively correlated metabolites were detected including MetO, malate, citrate, fumarate and argininosuccinate (cluster 1), Met, Ala, His, Thr, Pro, 4-hydroxyproline, Val, Leu, Ile, Phe, Tyr, Trp (cluster 2), and Asp. Glu, and Lys (cluster 3) (Fig. S3A†). Body levels of lactate, carnitine, GABA, and GSH negatively correlated with the levels of the cluster 1–3 metabolites (Fig. S3A†).

In nZnO-exposed mussels, concentrations of 22 metabolites were strongly positively correlated including argininosuccinate, malate, citrate, lactate, fumarate, pyruvate, Ala, Met, MetO, Val, Leu, Ile, Asn, Glu, Lys, Thr, Ser, His, Tyr, Phe, Trp, Pro, and 4-hydroxyproline (Fig. S3B†). Body levels of Gly, GABA, GSH and 2-oxoglutarate were negatively correlated with these metabolites (Fig. S3B†).

Pathway enrichment analysis showed that exposure to nZnO suppressed the metabolic rearrangement caused by hypoxia exposure in *M. edulis*. Thus, in control mussels, 14 pathways were significantly modulated by hypoxia while in nZnO-exposed mussels only six pathways were affected (FDR < 0.05) (Fig. 8A and B). The hypoxia-modulated pathways identified in both control and nZnO-exposed mussels included glutathione metabolism, butanoate metabolism, arginine and proline metabolism, arginine biosynthesis, D-glutamine and D-glutamate metabolism, and glyoxylate and dicarboxylate metabolism (Fig. 8A and B). Furthermore, in control mussels, hypoxia significantly altered the following pathways: cysteine and methionine metabolism, TCA cycle, alanine, aspartate, and glutamate metabolism, phenylalanine, tyrosine, and tryptophan biosynthesis, phenylalanine metabolism, purine metabolism, pyruvate metabolism, and biotin metabolism (Fig. 8A).

Exposure to nZnO hindered the metabolome recovery during post-hypoxic reoxygenation (Fig. 8C and D). In control mussels, six out of the 14 pathways affected by hypoxic exposure returned to the normoxic state after 24 h of recovery, including glutathione metabolism, arginine and proline metabolism, glyoxylate and dicarboxylate metabolism, purine metabolism, pyruvate metabolism, and biotin metabolism (Fig. 8A and C). Conversely, in nZnO-exposed mussels, post-hypoxic recovery led to further metabolic dysregulation, with significant alterations observed in 12 metabolic pathways relative to normoxia (Fig. 8B and D).

4. Discussion

4.1 nZnO alters mussel metabolism without causing energy deficit under normoxic conditions

Under normoxic condition, nZnO exposure did not impact the tissue energy content of *M. edulis* shown by the similarity of the content of proteins, lipids, carbohydrates and total energy reserves of the soft tissues. Furthermore, the CEA index was higher in the nZnO-exposed mussels compared to their control counterparts reflecting lower ETS activity, indicative of a diminished basal tissue energy demand. Prior investigations involving *M. edulis* exposed to 10 or 100 μg Zn L^{-1} of nZnO also corroborate these findings, showing either a lack of change or even a modest increase in CEA. Notably, outcomes varied depending on factors such as seasonal variations, salinity levels, and temperature conditions of exposure.[56,78] In some nZnO-salinity or -temperature combinations, a decline in the total energy reserves was found, attributed to reduced lipid and glycogen content in the tissues.[56,78] However, this decrease was counteracted by a concurrent reduction in ETS activity, thereby maintaining CEA at relatively stable levels.[56,78] Accumulation of lactate in nZnO exposed mussels suggests activation of cytosolic glycolysis and is consistent with the significant alteration of glyoxylate and carboxylate metabolism shown by the pathway enrichment analysis. This may indicate a greater reliance on anaerobic ATP
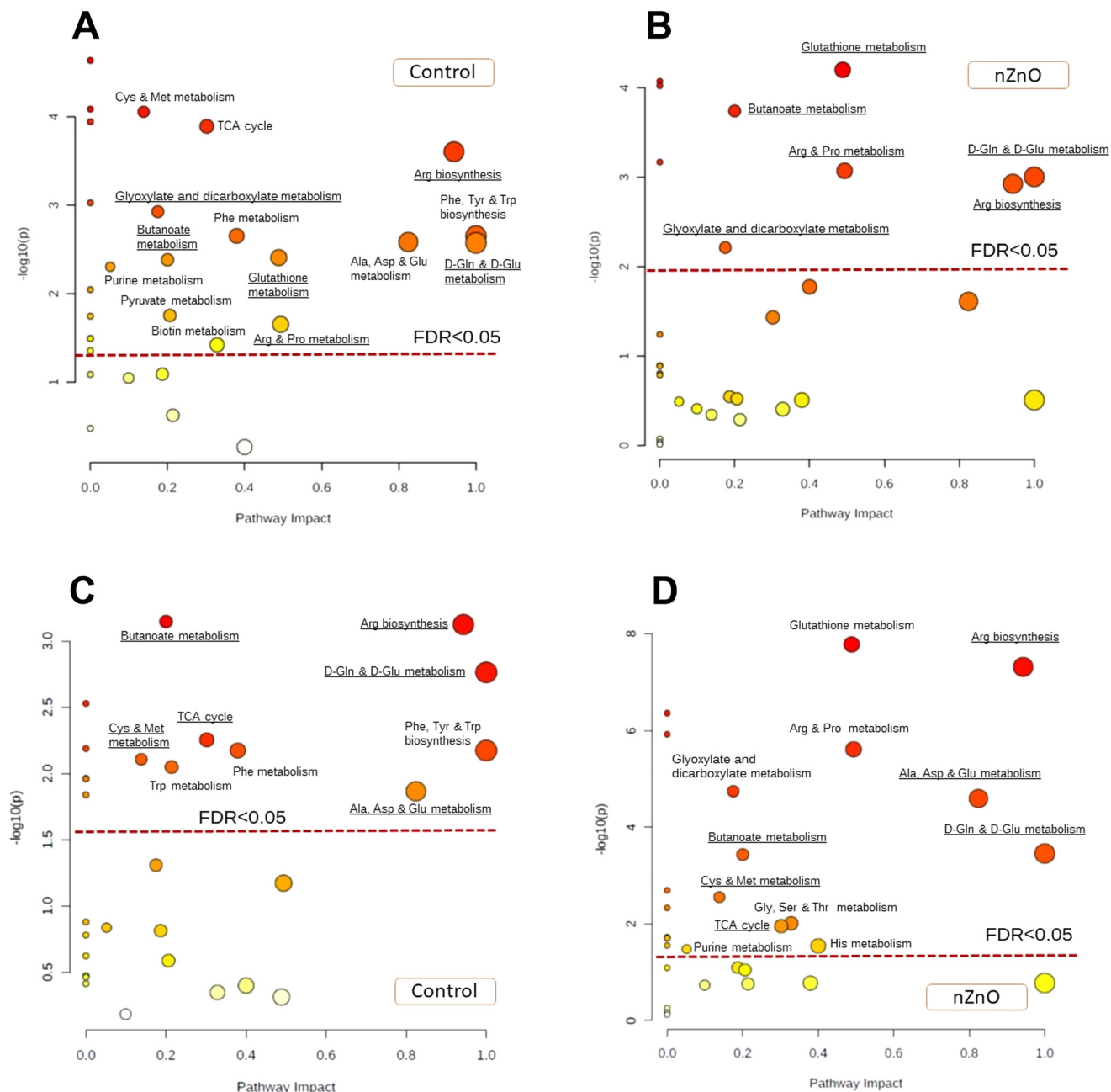
588 | *Environ. Sci.: Nano*, 2025, **12**, 576–596

This journal is © The Royal Society of Chemistry 2025

Fig. 8 Pathway enrichment analysis of the soft tissues of control and nZnO-exposed mussels in response to hypoxia and reoxygenation. A and C – Control mussels, B and D – nZnO-exposed mussels. Oxygen regimes: A and B – hypoxia, C and D – reoxygenation. Red broken line indicates the FDR cut-off of less than 0.05. Only pathways above this line are considered significantly altered (FDR < 0.05). The pathways with the impact >0 that are significantly altered in hypoxia-exposed mussels (A and B) or in recovering mussels (C and D) relative to the respective normoxic controls are labeled.

production to compensate for lower ETS activity in nZnO exposed mussels relative to the control counterparts. Taken together, these findings indicate that bioenergetics perturbations caused by environmentally relevant concentrations of nZnO might lead to a decrease in the cellular basal aerobic metabolism but do not induce significant energy misbalance in *M. edulis* tissues.

Notably, exposure to nZnO elicited contrasting effects on the activity of mitochondrial ETS and the mitochondrial matrix enzyme, CS, important in regulating the TCA cycle. A decrease in ETS activity along with elevated CS activity suggests a shift in mitochondrial metabolism from ATP synthesis towards biosynthesis due to nZnO exposure. This change appears to stem from the functional changes in the activities of the respective enzymes rather than by the shifts in the mitochondrial abundance as the mtDNA copy number was not affected by nZnO exposure in normoxic mussels. CS, encoded by

This journal is © The Royal Society of Chemistry 2025

Environ. Sci.: Nano, 2025, **12**, 576–596 | **589**

nuclear DNA, catalyzes a rate-controlling step in the TCA cycle and is subject to regulation by product inhibition (citrate), substrate availability (oxaloacetate), and allosteric inhibition by NADH.[79] While direct measurements of tissue levels of oxaloacetate or NADH were not conducted in this study, the diminished ETS activity (and thus lower rates of NADH oxidation) and elevated (iso)citrate levels in nZnO-exposed mussels under normoxic conditions would suggest inhibition rather than stimulation of CS activity, if these regulatory mechanisms were at play. Thus, the increased CS activity in nZnO-exposed mussels likely reflects elevated enzyme concentrations. Furthermore, the observed elevation in multiple TCA intermediates, including succinate, fumarate, (iso)citrate, malate, and 2-oxoglutarate, indicates an overall enhancement of TCA flux in nZnO-exposed mussels compared to their control counterparts under normoxic conditions. This notion finds support in the significant alteration of the TCA cycle in nZnO-exposed mussels identified by the pathway enrichment analysis. Alterations of TCA cycle were also reported in an annelid *A. marina* exposed to nZnO-spiked sediments (100 and 1000 μg Zn kg^{-1}); however, unlike in mussels, tissue levels of succinate and 2-oxoglutarate declined whereas fumarate concentrations increased in nZnO-exposed *A. marina*.[49] Taken together, these findings highlight the significance of TCA cycle as a crucial target of nZnO toxicity, while also suggesting that the varying effects observed in mussels and polychaetes may stem from species-specific sensitivities of TCA cycle enzymes to this nanopollutant.

nZnO exposure under normoxia also led to significant alteration of glutathione metabolism owing to a decrease in the concentrations of GSH and Gly. A decrease in Gly concentration in the body wall and the coelomic fluid has also been reported in a marine annelid *A. marina* exposed to nZnO-spiked sediment (100 and 1000 μg Zn kg^{-1}).[49] Gly is a precursor of GSH, so that a concomitant decrease in Gly and GSH in the tissues of nZnO-exposed mussels likely reflects a decrease in biosynthesis of this important antioxidant.[80] In contrast to Gly, an increase in the levels of several essential (Leu, Phe, Trp, His) and non-essential (Ala, Pro, Arg, Ser) amino acids was found under the normoxic conditions in nZnO-exposed *M. edulis*. The physiological implications of this increase are not clear, and the total levels of FAAs did not change in response to nZnO exposure. Conversely, in the lugworm *A. marina* nZnO exposure led to a decrease in tissue levels of multiple amino acids.[49] Owing to the limited amount of data on metabolome rearrangements caused by nZnO in marine organisms, no generalization is yet possible. However, the presence of nZnO-induced metabolic alterations, even in the absence of other stressors, underscores the critical need to continue assessing the metabolome disturbances induced by nZnO in marine organisms and to incorporate a broader range of taxonomically divergent groups in these assessments.

4.2 nZnO exposure disrupts metabolic response to hypoxia in mussels

Severe hypoxia (<0.1% air saturation) triggered anaerobic metabolism in *M. edulis*, evidenced by alanine and succinate accumulation alongside depletion of aspartate and glycogen in mussel tissues. This suggests activation of high-efficiency ATP production pathways (aspartate-succinate and glucose-succinate pathways) for anoxia survival in hypoxia-exposed mussels.[81] Notably, during severe hypoxia, mussels ceased feeding, so the observed metabolic and bioenergetic responses could be a combined effect of both hypoxia and accompanying starvation stress. Alanine accumulation, indicating early cytosolic anaerobiosis, was observed after 1 d of hypoxia exposure, followed by succinate accumulation, indicative of deep mitochondrial anaerobiosis, on day 7. Interestingly, activity of CS was upregulated during hypoxia in control mussels, without concomitant increase of (iso)citrate. It is therefore tempting to speculate that CS may catalyze the reverse reaction to support anaerobic succinate formation in hypoxia-exposed mussels, similar to TCA reversal mechanism observed in some anaerobic bacteria.[82–84] This speculation is supported by the requirement for high CS activity in the TCA cycle reversal observed in anaerobic bacteria,[82] a condition that would also be fulfilled by the observed hypoxia-induced increase in CS activity in mussels. However, the reversibility of CS activity in facultative animal anaerobes remains speculative and warrants further investigation, analogous to previous discoveries regarding succinate dehydrogenase reversibility in this animal group.[25,85,86]

Exposure to severe hypoxia induced a stronger anaerobic metabolic response in nZnO-exposed mussels as indicated by the higher alanine and succinate accumulation compared to control mussels. Additionally, the rapid accumulation of lactate after just 1 d of hypoxia in nZnO-exposed mussels suggests activation of the low efficiency/high rate ATP production lactate pathway.[81] Furthermore, alongside glycogen depletion, a reduction in tissue lipid content was observed in nZnO-exposed mussels after 7 d of hypoxia, indicating the involvement of fatty acids in anaerobic ATP production in this group.[20,87,88] Collectively, these findings suggest higher ATP turnover rates (and thus a reduced capacity for metabolic rate suppression) during hypoxia in nZnO-exposed mussels. This inability to depress anaerobic ATP turnover may compromise the anoxic survival of the mussels, as shown by a considerably higher mortality rate among nZnO-exposed mussels (63% after 7 d of hypoxia) compared to control mussels, of which only 28% died after 7 d in severe hypoxia. Interestingly, while control mussels exhibited increased CS activity under hypoxic conditions, CS activity was suppressed in hypoxic nZnO-exposed mussels. Since the forward TCA cycle is not involved in the anaerobic metabolism of marine bivalves,[20,89] the implications of this differential modulation of CS activity by hypoxia in control

590 | *Environ. Sci.: Nano*, 2025, **12**, 576–596

This journal is © The Royal Society of Chemistry 2025

and nZnO-exposed mussels are presently unclear and require further investigation.

In both control and nZnO-exposed mussels, a decline in mtDNA copy number was observed following prolonged (7 d) exposure to hypoxia. Previous studies have suggested an upregulation of autophagy and mitophagy in mussels during prolonged hypoxia,[23] potentially contributing to the observed decrease in mitochondrial DNA abundance. While the physiological implications of this reduction in mtDNA copy number in mussels remain uncertain, parallels can be drawn to findings in humans and other mammals, where decreased mtDNA copy numbers have been linked to conditions such as ischemia, neurodegenerative diseases, and mitochondrial disorders, leading to impaired mitochondrial function and ATP production.[90–92] In mussels, this decrease in mtDNA copy number appears to be transient, with full restoration observed after 24 h of reoxygenation, regardless of nZnO exposure. Interestingly, the tissue ETS activity remains unaffected by H–R exposure in mussels, suggesting that the dynamic regulation of the mitochondrial genome does not significantly impact mitochondrial respiratory capacity during H–R stress in these organisms. This underscores the remarkable plasticity of mussel aerobic metabolism in response to oxygen fluctuations.[35,93,94]

Hypoxia-induced metabolic rearrangements in the control mussels resulted in notable modifications across 14 pathways associated with energy metabolism, carbohydrate metabolism, amino acid metabolism, as well as co-factor metabolism involving glutathione (GSH) and biotin. During prolonged hypoxia, several key amino acids, including Ser, Lys, and Gln, were depleted, while others, such as Glu, Met, Val, Leu, Ile, and Phe, accumulated. Similar shifts in the content of FAAs were found in the gill tissues of M. edulis after 1 and 6 d of hypoxia, except for Ser and Lys that accumulated in the gills[29] but decreased in the whole body of the mussels (this study). The accumulation of Glu, along with decreased Gln levels, may suggest an ammonia overload surpassing the capacity of glutamine synthetase for conversion to Gln.[29,95,96] This imbalance might prompt the activation of the urea cycle, as indicated by elevated ornithine levels, to facilitate the removal of excess ammonia in hypoxia-exposed mussels. This mechanism appears to be active in both control and nZnO-exposed M. edulis. However, in nZnO-exposed mussels, fewer metabolic pathways were impacted by hypoxia exposure compared to the control mussels. Thus, no hypoxia-induced alterations were observed in the metabolism of aromatic amino acids (including Phe, Tyr, Trp metabolism, and biosynthesis), Cys and Met metabolism, as well as in TCA cycle, pyruvate, or biotin metabolism. This phenomenon may stem from the fact that many of the metabolic intermediates involved in the normal metabolic response to hypoxia in control mussels (including TCA and urea cycle intermediates, aromatic and branched-chain amino acids) are upregulated already in normoxia in nZnO-exposed mussels (cf. Fig. 8A and S2B†). Our analysis revealed no distinct pathways responding uniquely to hypoxia

in nZnO-exposed mussels that were not observed in the control group. This suggests that nZnO exposure truncates the typical metabolic response to hypoxia rather than activating novel metabolic pathways in M. edulis.

4.3 nZnO exposure hinders post-hypoxic recovery

Despite the significant hypoxia-induced metabolic shifts, the metabolic profiles of the control mussels swiftly recover upon reoxygenation. Glycogen and aspartate tissue levels, crucial substrates for anaerobic ATP production during hypoxia, were restored within 1 h of reoxygenation, with a notable surplus in aspartate accumulation after 24 h. Fumarate concentration exhibited a transient increase after 1 h of reoxygenation, indicative of active succinate oxidation. This observation aligns with prior research indicating enhanced mitochondrial capacity for succinate oxidation during the initial stages (minutes to hours) of post-hypoxic recovery in marine bivalves.[35,97–99] As a result, succinate concentrations returned to baseline levels after 24 h of post-hypoxic recovery in control mussels. Furthermore, CS activity increased after 1 and 24 h of reoxygenation, accompanied by the accumulation of (iso)citrate and 2-oxoglutarate, signaling the activation of the oxidative (forward) TCA cycle. These findings indicate a rapid reprogramming of mitochondrial metabolism towards aerobic pathways and the restoration of energy status during post-hypoxic recovery in M. edulis.

In contrast, in nZnO-exposed mussels, the recovery of glycogen stores was significantly delayed, with no observable recovery even after 24 h of reoxygenation. Additionally, there was no overshoot in aspartate accumulation after 24 h of recovery, and the reactivation of the TCA cycle was delayed, as shown by the absence of excess CS activation, lower than baseline levels of (iso)citrate, and slow metabolism of succinate, which did not return to baseline levels after 24 h of recovery. These findings indicate the deleterious effects of nZnO exposure on post-hypoxic recovery of energy homeostasis in M. edulis. The delayed recovery observed in mussels exposed to nZnO may be linked to increased rates of anaerobic metabolism, including less efficient lactate-producing glycolysis during hypoxia. This suggests that nZnO exposure could impair the mussels' ability to effectively suppress their metabolic rate – a key strategy for anaerobic survival – potentially due to the higher energy costs associated with nZnO detoxification and repair. Consequently, mussels exposed to nZnO exhibit greater accumulation of anaerobic byproducts and a more significant depletion of energy reserves during hypoxia, leading to a longer recovery time once oxygen levels return. Further research is needed to elucidate the mechanisms behind the metabolic disruption caused by nZnO in mussels and to determine whether similar effects occur in other marine organisms, particularly those capable of facultative anaerobiosis like mussels.

The hypoxia-induced shifts in tissue concentrations of free amino acids and urea cycle intermediates rapidly normalized following reoxygenation in the control mussels. Integration

This journal is © The Royal Society of Chemistry 2025

Environ. Sci.: Nano, 2025, 12, 576–596 | 591

of all studied metabolites through PCA analysis revealed that after 24 h of recovery, the metabolite profiles of control mussels nearly mirrored the normal, normoxic baseline. However, certain pathways remained altered in the recovering mussels compared to their normoxic counterparts, suggesting that 24 h was insufficient for complete restoration of metabolic homeostasis following prolonged (7 d) hypoxia. Notably, the metabolism of aromatic amino acids and metabolites involved in ammonium detoxification and nitrogen excretion (Gln, Glu, and Arg) remained perturbed in recovering control mussels. We observed elevated levels of Ser, likely reflecting slower Gly biosynthesis, a decrease in Glu concentrations associated with an increase in Gln, indicating restoration of Gln-dependent ammonia detoxification,[96,100] and heightened levels of branched-chain amino acids (Val, Ile, Leu), and the aromatic amino acid Phe in recovering control mussels. Additionally, tissue levels of Met, an amino acid involved in ROS scavenging,[101–103] were elevated during recovery, possibly serving as a protective mechanism against oxidative stress, as indicated by the accumulation of MetO after 24 h of reoxygenation in the control mussels.

In nZnO-exposed mussels, PCA analysis failed to indicate any restoration of the metabolite profile to its normoxic state, while pathway enrichment analysis revealed multiple disrupted metabolic pathways. Compared to controls, recovering nZnO-exposed mussels exhibited perturbations in twelve metabolic pathways, surpassing the nine observed in controls. Notably, tissue levels of Ser, Gly, Glu, Gln, Lys, Met, carnitine, and urea cycle intermediates Arg, ornithine, and argininosuccinate were significantly altered during recovery in nZnO-exposed mussels relative to the normoxic baseline. These findings underscore ongoing metabolic disturbances during post-hypoxic recovery in these mussels. The impaired recovery ability was further evidenced by the continued mortality of nZnO-exposed mussels (11% during 24 h of reoxygenation), in contrast to control mussels, all of which survived the 24 h recovery period. Our recent study also showed that nZnO synergistically enhances the immunosuppressive effects of hypoxia in *M. edulis* and delays the restoration of immune function following reoxygenation.[57] Given the high energy demand of immune cells[104,105] and the importance of amino acids for innate immunity,[106,107] the disturbances of the energy and amino acid metabolism observed in our present study may contribute to the immune dysregulation in mussels during combined exposures to fluctuating oxygen levels and nanopollutants,[57] which are common in eutrophicated and polluted coastal environments.

4.4 Conclusions, limitations, and outlook

Our study demonstrated the complex bioenergetics and metabolic responses of *M. edulis* to nZnO exposure and hypoxia, shedding light on the interactive effects of multiple environmental stressors on marine organisms. We found that

nZnO exposure disrupts energy metabolism, exacerbating hypoxia-induced metabolic stress and impairing post-hypoxic recovery in mussels. These findings emphasize the vulnerability of keystone marine species to nanoparticle toxicity and demonstrate that habitat dissolved oxygen must be considered in the biomarker-based assessment of nanoparticle toxicity in coastal ecosystems. However, while we conducted comprehensive metabolic profiling, further investigations are needed to elucidate the molecular mechanisms underlying nZnO toxicity and metabolic disruption in *M. edulis*. Future research should aim to integrate multi-omics approaches, including genomics, transcriptomics, and proteomics, to identify the molecular pathways mediating nanoparticle toxicity and metabolic adaptation in marine organisms. Additionally, our study underscores the importance of considering interactive effects of multiple stressors in ecotoxicological assessments. Anthropogenic activities continue to intensify in coastal regions, necessitating holistic approaches to understand and mitigate the ecological consequences of pollution and climate change.

Data availability

Data for this article, including raw data for all measured traits, are available at Zenodo repository, DOI https://zenodo.org/records/13165708.

Conflicts of interest

There are no conflicts to declare.

Acknowledgements

References

1 F. Borgwardt, L. Robinson, D. Trauner, H. Teixeira, A. J. A. Nogueira, A. I. Lillebø, G. Piet, M. Kuemmerlen, T. O'Higgins, H. McDonald, J. Arevalo-Torres, A. L. Barbosa, A. Iglesias-Campos, T. Hein and F. Culhane, Exploring variability in environmental impact risk from human activities across aquatic ecosystems, *Sci. Total Environ.*, 2019, **652**, 1396–1408.

2 P. M. Glibert, W.-J. Cai, E. R. Hall, M. Li, K. L. Main, K. A. Rose, J. M. Testa and N. K. Vidyarathna, Stressing over the

592 | *Environ. Sci.: Nano*, 2025, **12**, 576–596

This journal is © The Royal Society of Chemistry 2025

Complexities of Multiple Stressors in Marine and Estuarine Systems, *Ocean-Land-Atmos. Res.*, 2022, **2022**, 9787258.

3 M. M. Whitney, Observed and projected global warming pressure on coastal hypoxia, *Biogeosciences*, 2022, **19**, 4479–4497.

4 N. Gruber, Warming up, turning sour, losing breath: ocean biogeochemistry under global change, *Philos. Trans. R. Soc., A*, 2011, **369**, 1980–1996.

5 D. J. Conley, J. Carstensen, J. Aigars, P. Axe, E. Bonsdorff, T. Eremina, B.-M. Haahti, C. Humborg, P. Jonsson, J. Kotta, C. Lännegren, U. Larsson, A. Maximov, M. R. Medina, E. Lysiak-Pastuszak, N. Remeikaité-Nikiené, J. Walve, S. Wilhelms and L. Zillén, Hypoxia is increasing in the coastal zone of the Baltic Sea, *Environ. Sci. Technol.*, 2011, **45**, 6777–6783.

6 H. Ma, P. L. Williams and S. A. Diamond, Ecotoxicity of manufactured ZnO nanoparticles – A review, *Environ. Pollut.*, 2013, **172**, 76–85.

7 S. Yuan, J. Huang, X. Jiang, Y. Huang, X. Zhu and Z. Cai, Environmental Fate and Toxicity of Sunscreen-Derived Inorganic Ultraviolet Filters in Aquatic Environments: A Review, *Nanomaterials*, 2022, **12**(4), 699.

8 O. Bondarenko, K. Juganson, A. Ivask, K. Kasemets, M. Mortimer and A. Kahru, Toxicity of Ag, CuO and ZnO nanoparticles to selected environmentally relevant test organisms and mammalian cells in vitro: A critical review, *Arch. Toxicol.*, 2013, **87**, 1181–1200.

9 V. D. Rajput, T. M. Minkina, A. Behal, S. N. Sushkova, S. Mandzhieva, R. Singh, A. Gorovtsov, V. S. Tsitsuashvili, W. O. Purvis, K. A. Ghazaryan and H. S. Movsesyan, Effects of zinc-oxide nanoparticles on soil, plants, animals and soil organisms: A review, *Environ. Nanotechnol., Monit. Manage.*, 2018, **9**, 76–84.

10 C. M. Crain, K. Kroeker and B. S. Halpern, Interactive and cumulative effects of multiple human stressors in marine systems, *Ecol. Lett.*, 2008, **11**, 1304–1315.

11 I. M. Sokolova, M. Frederich, R. Bagwe, G. Lannig and A. A. Sukhotin, Energy homeostasis as an integrative tool for assessing limits of environmental stress tolerance in aquatic invertebrates, *Mar. Environ. Res.*, 2012, **79**, 1–15.

12 I. Sokolova, Bioenergetics in environmental adaptation and stress tolerance of aquatic ectotherms: linking physiology and ecology in a multi-stressor landscape, *J. Exp. Biol.*, 2021, **224**, jeb236802.

13 M. C. Lee, J. C. Park and J. S. Lee, Effects of environmental stressors on lipid metabolism in aquatic invertebrates, *Aquat. Toxicol.*, 2018, **200**, 83–92.

14 N. D. Wagner, B. P. Lankadurai, M. J. Simpson, A. J. Simpson and P. C. Frost, Metabolomic Differentiation of Nutritional Stress in an Aquatic Invertebrate, *Physiol. Biochem. Zool.*, 2015, **88**, 43–52.

15 E. D. Carlton, C. L. Cooper and G. E. Demas, Metabolic stressors and signals differentially affect energy allocation between reproduction and immune function, *Gen. Comp. Endocrinol.*, 2014, **208**, 21–29.

16 R. P. Ellis, H. Parry, J. I. Spicer, T. H. Hutchinson, R. K. Pipe and S. Widdicombe, Immunological function in marine invertebrates: Responses to environmental perturbation, *Fish Shellfish Immunol.*, 2011, **30**, 1209–1222.

17 P. A. Parsons, The metabolic cost of multiple environmental stresses: Implications for climatic change and conservation, *Trends Ecol. Evol.*, 1990, **5**, 315–317.

18 P. W. Hochachka and P. L. Lutz, Mechanism, origin, and evolution of anoxia tolerance in animals, *Comp. Biochem. Physiol., Part B: Biochem. Mol. Biol.*, 2001, **130**, 435–459.

19 P. W. Hochachka, P. L. Lutz, T. J. Sick and M. Rosenthal, *Surviving Hypoxia: Mechanisms of Control and Adaptation*, Taylor & Francis, 1993.

20 M. Müller, M. Mentel, J. J. van Hellemond, K. Henze, C. Woehle, S. B. Gould, R.-Y. Yu, M. van der Giezen, A. G. M. Tielens and W. F. Martin, Biochemistry and Evolution of Anaerobic Energy Metabolism in Eukaryotes, *Microbiol. Mol. Biol. Rev.*, 2012, **76**, 444–495.

21 H. Pörtner, Contributions of anaerobic metabolism to pH regulation in animal tissues: theory, *J. Exp. Biol.*, 1987, **131**, 69–87.

22 T. Liu, Y. Lu, M. Sun, H. Shen and D. Niu, Effects of acute hypoxia and reoxygenation on histological structure, antioxidant response, and apoptosis in razor clam Sinonovacula constricta, *Fish Shellfish Immunol.*, 2024, **145**, 109310.

23 J. B. M. Steffen, H. I. Falfushynska, H. Piontkivska and I. M. Sokolova, Molecular Biomarkers of the Mitochondrial Quality Control Are Differently Affected by Hypoxia-Reoxygenation Stress in Marine Bivalves Crassostrea gigas and Mytilus edulis, *Front. Mar. Sci.*, 2020, **7**, 604411.

24 R. G. Boutilier and J. St-Pierre, Surviving hypoxia without really dying, *Comp. Biochem. Physiol., Part A: Mol. Integr. Physiol.*, 2000, **126**, 481–490.

25 M. K. Grieshaber, I. Hardewig, U. Kreutzer and H. O. Pörtner, Physiological and metabolic responses to hypoxia in invertebrates, *Rev. Physiol., Biochem. Pharmacol.*, 1994, **125**, 43–147.

26 A. Fago, New insights into survival strategies to oxygen deprivation in anoxia-tolerant vertebrates, *Acta Physiol.*, 2022, **235**, e13841.

27 I. M. Sokolova, E. P. Sokolov and F. Haider, Mitochondrial mechanisms underlying tolerance to fluctuating oxygen conditions: lessons from hypoxia-tolerant organisms, *Integr. Comp. Biol.*, 2019, **59**, 938–952.

28 T. Bruhns, S. Timm, N. Feußner, S. Engelhaupt, M. Labrenz, M. Wegner and I. M. Sokolova, Combined effects of temperature and emersion-immersion cycles on metabolism and bioenergetics of the Pacific oyster Crassostrea (Magallana) gigas, *Mar. Environ. Res.*, 2023, **192**, 106231.

29 F. Haider, H. I. Falfushynska, S. Timm and I. M. Sokolova, Effects of hypoxia and reoxygenation on intermediary metabolite homeostasis of marine bivalves Mytilus edulis and Crassostrea gigas, *Comp. Biochem. Physiol., Part A: Mol. Integr. Physiol.*, 2020, **242**, 110657.

30 A. V. Ivanina, B. Froelich, T. Williams, E. P. Sokolov, J. D. Oliver and I. M. Sokolova, Interactive effects of cadmium and hypoxia on metabolic responses and bacterial loads of eastern oysters Crassostrea virginica Gmelin, Chemosphere, 2011, 82, 377–389.

31 W. R. Ellington, The recovery from anaerobic metabolism in invertebrates, J. Exp. Zool., 1983, 228, 431–444.

32 B. Vismann and L. Hagerman, Recovery from hypoxia with and without sulfide in Saduria entomon: Oxygen debt, reduced sulfur and anaerobic metabolites, Mar. Ecol.: Prog. Ser., 1996, 143, 131–139.

33 A. Bundgaard, A. M. James, A. V. Gruszczyk, J. Martin, M. P. Murphy and A. Fago, Metabolic adaptations during extreme anoxia in the turtle heart and their implications for ischemia-reperfusion injury, Sci. Rep., 2019, 9, 2850.

34 H. Falfushynska and I. M. Sokolova, Intermittent hypoxia differentially affects metabolic and oxidative stress responses in two species of cyprinid fish, Biol. Open, 2023, 12, bio060069.

35 E. P. Sokolov, L. Adzigbli, S. Markert, A. Bundgaard, A. Fago, D. Becher, C. Hirschfeld and I. M. Sokolova, Intrinsic mechanisms underlying hypoxia-tolerant mitochondrial phenotype during hypoxia-reoxygenation stress in a marine facultative anaerobe, the blue mussel Mytilus edulis, Front. Mar. Sci., 2021, 8, 773734.

36 C. Casals-Casas and B. Desvergne, Endocrine Disruptors: From Endocrine to Metabolic Disruption, Annu. Rev. Physiol., 2011, 73, 135–162.

37 B. Le Magueresse-Battistoni, H. Vidal and D. Naville, Environmental Pollutants and Metabolic Disorders: The Multi-Exposure Scenario of Life, Front. Endocrinol., 2018, 9, 582.

38 C. J. Dedman, Nano-ecotoxicology in a changing ocean, SN Appl. Sci., 2022, 4, 264.

39 C. Coll, D. Notter, F. Gottschalk, T. Y. Sun, C. Som and B. Nowack, Probabilistic environmental risk assessment of five nanomaterials (nano-TiO$_2$, nano-Ag, nano-ZnO, CNT, and fullerenes), Nanotoxicology, 2016, 10, 436–444.

40 H. Hong, V. Adam and B. Nowack, Form-Specific and Probabilistic Environmental Risk Assessment of Three Engineered Nanomaterials (nano-Ag, nano-TiO2 and nano-ZnO) in European Freshwaters, Environ. Toxicol. Chem., 2021, 40, 2629–2639.

41 E. Dumont, A. C. Johnson, V. D. J. Keller and R. J. Williams, Nano silver and nano zinc-oxide in surface waters – Exposure estimation for Europe at high spatial and temporal resolution, Environ. Pollut., 2015, 196, 341–349.

42 F. Gottschalk, T. Sun and B. Nowack, Environmental concentrations of engineered nanomaterials: Review of modeling and analytical studies, Environ. Pollut., 2013, 181, 287–300.

43 A. Boxall, Q. Chaudhry, C. Sinclair, A. Jones, R. Aitken, B. Jefferson and C. Watts, Current and future predicted environmental exposure to engineered nanoparticles, Central Science Laboratory, York, UK, 2007.

44 R. Miller, A. Adeleye, H. Page, L. Kui, H. Lenihan and A. Keller, Nano and traditional copper and zinc antifouling coatings: metal release and impact on marine sessile invertebrate communities, J. Nanopart. Res., 2020, 22, 129.

45 I. Efthimiou, G. Kalamaras, K. Papavasileiou, N. Anastasi-Papathanasi, Y. Georgiou, S. Dailianis, Y. Deligiannakis and D. Vlastos, ZnO, Ag and ZnO-Ag nanoparticles exhibit differential modes of toxic and oxidative action in hemocytes of mussel Mytilus galloprovincialis, Sci. Total Environ., 2021, 767, 144699.

46 F. Wu, E. P. Sokolov, A. Khomich, C. Fettkenhauer, G. Schnell, H. Seitz and I. M. Sokolova, Interactive effects of ZnO nanoparticles and temperature on molecular and cellular stress responses of the blue mussel Mytilus edulis, Sci. Total Environ., 2022, 818, 151785.

47 L. Cui, X. Wang, B. Sun, T. Xia and S. Hu, Predictive Metabolomic Signatures for Safety Assessment of Metal Oxide Nanoparticles, ACS Nano, 2019, 13, 13065–13082.

48 P. Kumar Babele, Zinc oxide nanoparticles impose metabolic toxicity by de-regulating proteome and metabolome in Saccharomyces cerevisiae, Toxicol. Rep., 2019, 6, 64–73.

49 T. Bruhns, S. Timm and I. M. Sokolova, Metabolomics-based assessment of nanoparticles (nZnO) toxicity in an infaunal marine annelid, the lugworm Arenicola marina (Annelida: Sedentaria), Sci. Total Environ., 2023, 858, 160039.

50 C. Faggio, V. Tsarpali and S. Dailianis, Mussel digestive gland as a model tissue for assessing xenobiotics: An overview, Sci. Total Environ., 2018, 636, 220–229.

51 L. Canesi, C. Ciacci, R. Fabbri, A. Marcomini, G. Pojana and G. Gallo, Bivalve molluscs as a unique target group for nanoparticle toxicity, Mar. Environ. Res., 2011, 76, 16–21.

52 W. M. De Coen and C. R. Janssen, The use of biomarkers in Daphnia magna toxicity testing. IV. Cellular Energy Allocation: a new methodology to assess the energy budget of toxicant-stressed Daphnia populations, J. Aquat. Ecosyst. Stress Recovery, 1997, 6, 43–55.

53 M. Van Dievel, L. Janssens and R. Stoks, Additive bioenergetic responses to a pesticide and predation risk in an aquatic insect, Aquat. Toxicol., 2019, 212, 205–213.

54 V. V. Khlebovich, Acclimation of animal organisms: basic theory and applied aspects, Biol. Bull. Rev., 2017, 7, 279–286.

55 E. L. Thompson, D. A. Taylor, S. V. Nair, G. Birch, R. Coleman and D. A. Raftos, Optimal acclimation periods for oysters in laboratory-based experiments, J. Molluscan Stud., 2012, 78, 304–307.

56 F. Wu, E. P. Sokolov, O. Dellwig and I. M. Sokolova, Season-dependent effects of ZnO nanoparticles and elevated temperature on bioenergetics of the blue mussel Mytilus edulis, Chemosphere, 2021, 263, 127780.

57 F. Wu, H. Kong, L. Xie and I. M. Sokolova, Exposure to nanopollutants (nZnO) enhances the negative effects of hypoxia and delays recovery of the mussels' immune system, Environ. Pollut., 2024, 351, 124112.

594 | Environ. Sci.: Nano, 2025, 12, 576–596

This journal is © The Royal Society of Chemistry 2025

58 D. J. Conley, J. Carstensen, J. Aigars, P. Axe, E. Bonsdorff, T. Eremina, B. M. Haahti, C. Humborg, P. Jonsson, J. Kotta, C. Lännegren, U. Larsson, A. Maximov, M. R. Medina, E. Lysiak-Pastuszak, N. Remeikaite-Nikiene, J. Walve, S. Wilhelms and L. Zillén, Hypoxia Is Increasing in the Coastal Zone of the Baltic Sea, *Environ. Sci. Technol.*, 2011, **45**, 6777–6783.

59 R. J. Diaz and R. Rosenberg, Spreading dead zones and consequences for marine ecosystems, *Science*, 2008, **321**, 926–929.

60 K. Fennel and J. M. Testa, in *Annual Review of Marine Science*, ed. C. A. Carlson and S. J. Giovannoni, 2019, vol. 11, pp. 105–130.

61 S. A. Jokinen, J. J. Virtasalo, T. Jilbert, J. Kaiser, O. Dellwig, H. W. Arz, J. Hänninen, L. Arppe, M. Collander and T. Saarinen, A 1500-year multiproxy record of coastal hypoxia from the northern Baltic Sea indicates unprecedented deoxygenation over the 20th century, *Biogeosciences*, 2018, **15**, 3975–4001.

62 F. Haider, H. I. Falfushynska, S. Timm and I. M. Sokolova, Effects of hypoxia and reoxygenation on intermediary metabolite homeostasis of marine bivalves Mytilus edulis and Crassostrea gigas, *Comp. Biochem. Physiol., Part A: Mol. Integr. Physiol.*, 2020, **242**, 110657.

63 T. N. Andrienko, P. Pasdois, G. C. Pereira, M. J. Ovens and A. P. Halestrap, The role of succinate and ROS in reperfusion injury - A critical appraisal, *J. Mol. Cell. Cardiol.*, 2017, **110**, 1–14.

64 A. V. Ivanina and I. M. Sokolova, Effects of intermittent hypoxia on oxidative stress and protein degradation in molluscan mitochondria, *J. Exp. Biol.*, 2016, **219**, 3794–3802.

65 I. M. Sokolova, E. P. Sokolov and F. Haider, Mitochondrial Mechanisms Underlying Tolerance to Fluctuating Oxygen Conditions: Lessons from Hypoxia-Tolerant Organisms, *Integr. Comp. Biol.*, 2019, **59**, 938–952.

66 P. B. Lobel, C. D. Bajdik, S. P. Belkhode, S. E. Jackson and H. P. Longerich, Improved protocol for collecting mussel watch specimens taking into account sex, size, condition, shell shape, and chronological age, *Arch. Environ. Contam. Toxicol.*, 1991, **21**, 409–414.

67 F. Haider, E. P. Sokolov and I. M. Sokolova, Effects of mechanical disturbance and salinity stress on bioenergetics and burrowing behavior of the soft-shell clam Mya arenaria, *J. Exp. Biol.*, 2018, **221**, jeb172643.

68 E. Van Handel, Rapid determination of total lipids in mosquitoes, *J. Am. Mosq. Control Assoc.*, 1985, **1**, 302–304.

69 T. Masuko, A. Minami, N. Iwasaki, T. Majima, S. I. Nishimura and Y. C. Lee, Carbohydrate analysis by a phenol-sulfuric acid method in microplate format, *Anal. Biochem.*, 2005, **339**, 69–72.

70 H. I. Falfushynska, F. L. Wu, F. Ye, N. Kasianchuk, J. Dutta, S. Dobretsov and I. M. Sokolova, The effects of ZnO nanostructures of different morphology on bioenergetics and stress response biomarkers of the blue mussels Mytilus edulis, *Sci. Total Environ.*, 2019, **694**, 133717.

71 W. M. DeCoen and C. R. Janssen, The use of biomarkers in Daphnia magna toxicity testing .2. Digestive enzyme activity in Daphnia magna exposed to sublethal concentrations of cadmium, chromium and mercury, *Chemosphere*, 1997, **35**, 1053–1067.

72 E. Gnaiger, in *Polarographic Oxygen Sensors: Aquatic and Physiological Applications*, ed. E. Gnaiger and H. Forstner, Springer Berlin Heidelberg, Berlin, Heidelberg, 1983, pp. 337–345, DOI: 10.1007/978-3-642-81863-9_30.

73 T. Verslycke, S. D. Roast, J. Widdows, M. B. Jones and C. R. Janssen, Cellular energy allocation and scope for growth in the estuarine mysid Neomysis integer (Crustacea: Mysidacea) following chlorpyrifos exposure: a method comparison, *J. Exp. Mar. Biol. Ecol.*, 2004, **306**, 1–16.

74 P. A. Srere, H. Brazil and L. Gonen, The citrate condensing enzyme of pigeon breast muscle and moth flight muscle, *Acta Chem. Scand.*, 1963, **17**, 129–134.

75 M. M. H. Mredul, E. P. Sokolov, H. Kong and I. M. Sokolova, Spawning acts as a metabolic stressor enhanced by hypoxia and independent of sex in a broadcast marine spawner, *Sci. Total Environ.*, 2024, **909**, 168419.

76 L. M. Fitzgerald and A. M. Szmant, Biosynthesis of 'essential' amino acids by scleractinian corals, *Biochem. J.*, 1997, **322**(Pt 1), 213–221.

77 Z. Pang, J. Chong, G. Zhou, D. A. de Lima Morais, L. Chang, M. Barrette, C. Gauthier, P.-É. Jacques, S. Li and J. Xia, MetaboAnalyst 5.0: narrowing the gap between raw spectra and functional insights, *Nucleic Acids Res.*, 2021, **49**, W388–W396.

78 M. N. Noor, F. Wu, E. P. Sokolov, H. Falfushynska, S. Timm, F. Haider and I. M. Sokolova, Salinity-dependent effects of ZnO nanoparticles on bioenergetics and intermediate metabolite homeostasis in a euryhaline marine bivalve, Mytilus edulis, *Sci. Total Environ.*, 2021, **774**, 145195.

79 P. K. Arnold and L. W. S. Finley, Regulation and function of the mammalian tricarboxylic acid cycle, *J. Biol. Chem.*, 2023, **299**, 102838.

80 M. A. Razak, P. S. Begum, B. Viswanath and S. Rajagopal, Multifarious Beneficial Effect of Nonessential Amino Acid, Glycine: A Review, *Oxid. Med. Cell. Longevity*, 2017, **2017**, 1716701.

81 D. R. Livingstone, Origins and evolution of pathways of anaerobic metabolism in the animal kingdom, *Am. Zool.*, 1991, **31**, 522–534.

82 L. Steffens, E. Pettinato, T. M. Steiner, W. Eisenreich and I. A. Berg, Tracking the Reversed Oxidative Tricarboxylic Acid Cycle in Bacteria, *Bio-Protoc.*, 2022, **12**, e4364.

83 T. Nunoura, Y. Chikaraishi, R. Izaki, T. Suwa, T. Sato, T. Harada, K. Mori, Y. Kato, M. Miyazaki, S. Shimamura, K. Yanagawa, A. Shuto, N. Ohkouchi, N. Fujita, Y. Takaki, H. Atomi and K. Takai, A primordial and reversible TCA cycle in a facultatively chemolithoautotrophic thermophile, *Science*, 2018, **359**, 559–563.

84 A. Mall, J. Sobotta, C. Huber, C. Tschirner, S. Kowarschik, K. Bačnik, M. Mergelsberg, M. Boll, M. Hügler, W.

This journal is © The Royal Society of Chemistry 2025

Environ. Sci.: Nano, 2025, **12**, 576–596 | 595

Eisenreich and I. A. Berg, Reversibility of citrate synthase allows autotrophic growth of a thermophilic bacterium, *Science*, 2018, **359**, 563–567.

85 L. T. Buck, Succinate and alanine as anaerobic end-products in the diving turtle (Chrysemys picta bellii), *Comp. Biochem. Physiol., Part B: Biochem. Mol. Biol.*, 2000, **126**, 409–413.

86 J. J. van Hellemond, A. van der Klei, S. W. H. van Weelden and A. G. M. Tielens, Biochemical and evolutionary aspects of anaerobically functioning mitochondria, *Philos. Trans. R. Soc., B*, 2003, **358**, 205–215.

87 S. L. Neave and A. M. Buswell, The anaerobic oxidation of fatty acids, *J. Am. Chem. Soc.*, 1930, **52**, 3308–3314.

88 P. W. Hochachka, J. Fields and T. Mustafa, Animal Life Without Oxygen: Basic Biochemical Mechanisms, *Am. Zool.*, 1973, **13**, 543–555.

89 J. M. Collicutt and P. W. Hochachka, The anaerobic oyster heart: Coupling of glucose and aspartate fermentation, *J. Comp. Physiol.*, 1977, **115**, 147–157.

90 B. G. Hill, G. A. Benavides, J. R. Lancaster, Jr., S. Ballinger, L. Dell'Italia, Z. Jianhua and V. M. Darley-Usmar, Integration of cellular bioenergetics with mitochondrial quality control and autophagy, *Biol. Chem.*, 2012, **393**, 1485–1512.

91 A. Pyle, H. Anugrha, M. Kurzawa-Akanbi, A. Yarnall, D. Burn and G. Hudson, Reduced mitochondrial DNA copy number is a biomarker of Parkinson's disease, *Neurobiol. Aging*, 2016, **38**, 216.

92 R. Filograna, M. Mennuni, D. Alsina and N.-G. Larsson, Mitochondrial DNA copy number in human disease: the more the better?, *FEBS Lett.*, 2021, **595**, 976–1002.

93 H. I. Falfushynska, E. Sokolov, H. Piontkivska and I. M. Sokolova, The Role of Reversible Protein Phosphorylation in Regulation of the Mitochondrial Electron Transport System During Hypoxia and Reoxygenation Stress in Marine Bivalves, *Front. Mar. Sci.*, 2020, **7**, 00467.

94 I. Georgoulis, K. Feidantsis, I. A. Giantsis, A. Kakale, C. Bock, H. O. Pörtner, I. M. Sokolova and B. Michaelidis, Heat hardening enhances mitochondrial potential for respiration and oxidative defence capacity in the mantle of thermally stressed Mytilus galloprovincialis, *Sci. Rep.*, 2021, **11**, 17098.

95 L. Y. Jow, S. F. Chew, S. B. Lim, P. M. Anderson and Y. K. Ip, The marble goby Oxyeleotris marmoratus activates hepatic glutamine synthetase and detoxifies ammonia to glutamine during air exposure, *J. Exp. Biol.*, 1999, **202**, 237–245.

96 K. C. Hiong, W. Y. X. Peh, A. M. Loong, W. P. Wong, S. F. Chew and Y. K. Ip, Exposure to air, but not seawater, increases the glutamine content and the glutamine synthetase activity in the marsh clam Polymesoda expansa, *J. Exp. Biol.*, 2004, **207**, 4605–4614.

97 J. B. M. Steffen, E. P. Sokolov, C. Bock and I. M. Sokolova, Combined effects of salinity and intermittent hypoxia on mitochondrial capacity and reactive oxygen species efflux in the Pacific oyster, Crassostrea gigas, *J. Exp. Biol.*, 2023, **226**, jeb246164.

98 L. Adzigbli, E. P. Sokolov, S. Ponsuksili and I. M. Sokolova, Tissue- and substrate-dependent mitochondrial responses to acute hypoxia–reoxygenation stress in a marine bivalve (Crassostrea gigas), *J. Exp. Biol.*, 2022, **225**, jeb243304.

99 E. P. Sokolov, S. Markert, T. Hinzke, C. Hirschfeld, D. Becher, S. Ponsuksili and I. M. Sokolova, Effects of hypoxia-reoxygenation stress on mitochondrial proteome and bioenergetics of the hypoxia-tolerant marine bivalve Crassostrea gigas, *J. Proteomics*, 2019, **194**, 99–111.

100 G. Hongxing, L. Xiafei, L. Jialing, C. Zhenquan, G. Luoyu, L. Lei, S. Yuxuan, D. Zhiguo and W. Min, Effects of acute ammonia exposure on antioxidant and detoxification metabolism in clam Cyclina sinensis, *Ecotoxicol. Environ. Saf.*, 2021, **211**, 111895.

101 K. Campbell, J. Vowinckel, M. A. Keller and M. Ralser, Methionine Metabolism Alters Oxidative Stress Resistance via the Pentose Phosphate Pathway, *Antioxid. Redox Signaling*, 2016, **24**, 543–547.

102 B. C. Lee, A. Dikiy, H. Y. Kim and V. N. Gladyshev, Functions and evolution of selenoprotein methionine sulfoxide reductases, *Biochim. Biophys. Acta, Gen. Subj.*, 2009, **1790**, 1471–1477.

103 R. L. Levine, L. Mosoni, B. S. Berlett and E. R. Stadtman, Methionine residues as endogenous antioxidants in proteins, *Proc. Natl. Acad. Sci. U. S. A.*, 1996, **93**, 15036–15040.

104 S. Chen, Z. Liao and P. Xu, Mitochondrial control of innate immune responses, *Front. Immunol.*, 2023, **14**, 1166214.

105 L. Lartigue and B. Faustin, Mitochondria: Metabolic regulators of innate immune responses to pathogens and cell stress, *Int. J. Biochem. Cell Biol.*, 2013, **45**, 2052–2056.

106 B. Kelly and E. L. Pearce, Amino Assets: How Amino Acids Support Immunity, *Cell Metab.*, 2020, **32**, 154–175.

107 P. Li, Y. L. Yin, D. Li, S. W. Kim and G. Wu, Amino acids and immune function, *J. Geophys. Res. Oceans*, 2007, **98**, 237–252.

596 | *Environ. Sci.: Nano*, 2025, **12**, 576–596

This journal is © The Royal Society of Chemistry 2025